



EMISSIONS OF TRAIN BRAKES CHARACTERIZED IN PARTICLE SIZE AND CHEMICAL COMPOSITION

WP3, TASK3.1

Date of document

29/08/2025

DELIVERABLE VERSION:

D3.1, V.3.2

DISSEMINATION LEVEL:

PU*

AUTHOR(S):

Christof Asbach¹, Stefan Schumacher¹, Max Weissbuch¹, Simon Schastok¹,
Stefanos Agathokleous², Teresa Moreno², Tomé Canas³, Sevdalina Voynova⁴
(¹IUTA, ²CSIC, ³Metro Lisbon, ⁴Metro Sofia)

* PU = Public - fully open

SEN = Sensitive - limited under the conditions of the Grant Agreement

EU classified — RESTREINT-UE/EU-RESTRICTED, CONFIDENTIEL-UE/EU-CONFIDENTIAL, SECRET-UE/EU-SECRET under Decision 2015/444

DOCUMENT HISTORY

PROJECT ACRONYM	AEROSOLFD		
Project Title	Fast track to cleaner, healthier urban Aerosols by market ready Solutions of retrofit Filtration Devices for tailpipe, brake systems and closed environment		
Grant Agreement N°	101056661		
Project Coordinator	M+H		
Project Duration	01/05/2022 – 31/08/2025 (40 Months)		
Deliverable No.	D3.1 - Emissions of train brakes characterized in particle size and chemical composition		
Diss. Level	Public (PU)		
Deliverable Lead	IUTA		
Status	Working Verified by other WPs/Partners X Final version		
Due date	30/04/2023		
Submission date	29/08/2025		
Work Package	WP 3 - Retrofit solutions for closed environments - Product Optimisation and Demonstration		
Work Package Lead	M+H		
Contributing beneficiaries	IUTA, Metro Lisbon, Metro Sofia, CSIC		
DoA	Emissions of train brakes characterized in particle size and chemical composition. This deliverable refers to task 3.1.		
DATE	VERSION	AUTHOR	COMMENT
2023/12/01	1	Christof Asbach	First draft of deliverable, containing only results for brakes from Metro Lisbon



2023/12/18	1.1	Christof Asbach	Revision after comments received from Max Weissbuch
2024/08/13	1.3	Max Weissbuch	Addition of chapters on measurements and results for brakes from Metro Sofia
2024/08/15	2	Christof Asbach	Finalisation of draft deliverable
2024/10/09	3	Christof Asbach	Finalisation of deliverable report after receiving comments from co-authors
2025/05/28	3.1	Katie Kedwell, Martin Lehmann	Final version with minor revisions.
2025/08/01	3.2	Christof Asbach	Corrections according to the PO's request in the rejection letter for V3.1

©2022-2025 AeroSolfd Consortium Partners. All rights reserved.

Funded by the European Union. Views and opinions expressed are however those of the author(s) only and do not necessarily reflect those of the European Union or the European Climate, Infrastructure and Environment Executive Agency (CINEA). Neither the European Union nor the granting authority can be held responsible for them.

AeroSolfd is a Horizon Europe project supported by the European Commission under grant agreement No 101056661. All information in this deliverable may not be copied or duplicated in whole or part by any means without express prior agreement in writing by the AeroSolfd partners. All contents are reserved by default and may not be disclosed to third parties without the written consent of the AeroSolfd partners, except as mandated by the Grant Agreement with the European Commission, for reviewing and dissemination purposes. All trademarks and other rights on third party products mentioned in this document are acknowledged and owned by the respective holders. The AeroSolfd consortium does not guarantee that any information contained herein is error-free, or up-to-date, nor makes warranties, express, implied, or statutory, by publishing this document. For more information on the project, its partners and contributors, please see the AeroSolfd website (www.aerosolfd-project.eu).

TABLE OF CONTENTS

1. INTRODUCTION	12
1.1. PURPOSE AND TARGET GROUP	13
1.2. CONTRIBUTIONS OF PARTNERS	13
2. OBJECTIVES AND EXPECTED IMPACT	14
2.1. OBJECTIVES OF D3.1	14
2.2. EXPECTED IMPACT	14
3. DESCRIPTION OF TECHNICAL/SCIENTIFIC ACTIVITIES	15
3.1. DEVELOPMENT OF A SAMPLING SYSTEM FOR CHARACTERIZING DUST EMISSIONS OF METRO BRAKES ON A DYNAMOMETER TEST RIG	15
3.2. MEASUREMENT EQUIPMENT	16
3.2.1. Direct reading measurement equipment	17
3.2.2. Filter samplers	17
3.3. MEASUREMENTS CARRIED OUT ON BRAKE FROM METRO LISBON	18
3.3.1. Measurement protocol	18
3.3.2. Results from Metro Lisbon	19
3.3.2.1. Driving cycle and resulting brake temperatures	19
3.3.2.2. Results from physical aerosol characterisation	21
3.3.2.3. Results from Chemical aerosol characterisation	24
3.3.3. Conclusions from measurements on brake from Metro Lisbon	26
3.4. MEASUREMENTS CARRIED OUT ON BRAKE FROM METRO SOFIA	27
3.4.1. Measurement Protocol	27
3.4.2. Results from metro sofia	29
3.4.2.1. Driving cycle and resulting brake temperatures	29
3.4.2.2. Results from physical aerosol characterisation	31
3.4.2.3. Results from Chemical aerosol characterisation	33
3.4.3. Conclusions from measurements on brake from metro sofia	36
3.5. POSSIBLE CONTRIBUTION OF BRAKE EMISSIONS TO WATER QUALITY AND DAMAGE TO HISTORIC BUILDINGS	36
4. DEVIATIONS FROM THE PLAN	39
5. LINKS WITH OTHER WPS	39
6. CONCLUSIONS AND RECOMMENDATIONS	40
7. BIBLIOGRAPHY	41



LIST OF TABLES

Table 1. Contribution of each partner in this deliverable 13

LIST OF FIGURES

Figure 1: 3D CAD drawings of the sampling system for the measurement of dust emitted from metro brakes..... 15

Figure 2: Photograph of the installed sampling system..... 16

Figure 3: Line map of the metro in Lisbon; the relevant blue line is marked with a blue ellipse and the demo site Alto dos Moinhos with a red ellipse (Source: <https://www.metrolisboa.pt/en/travel/diagrams-and-maps/>)..... 19

Figure 4: Driving speed (black), brake disc temperature (red) and friction coefficient (green) during a full return trip of the blue line using braking method A; first/last station Reboleira (red arrow), demo site Alto dos Moinhos (blue arrow), turnaround station Santa Apolonia (green arrow)..... 20

Figure 5: Driving speed (black), brake disc temperature (red) and friction coefficient (green) during a full round trip of the blue line using braking method B; first/last station Reboleira (red arrow), demo site Alto dos Moinhos (blue arrow), turnaround station Santa Apolonia (green arrow)..... 21

Figure 6: Average number size distribution of brake dust emitted from the brake from Metro Lisbon measured with FMPS and OPS using braking method A; average of all stops at the 17 stations during five round trips; error bars indicate the standard deviations of the concentrations in each particle size class. 22

Figure 7: Average number size distribution of brake dust emitted from the brake from Metro Lisbon measured with FMPS and OPS using braking method B; average of all stops at the 17 stations during 17 round trips; error bars indicate the standard deviations of the concentrations in each particle size class..... 23

Figure 8: Average particle number size distributions emitted by the brake from Metro Lisbon, measured applying method A (primary concentration axis) and method B (secondary concentration axis); background number size distribution subtracted for both..... 24

Figure 9: Average composition of PM_{2.5} emitted by the brakes from Metro Lisbon and collected on filters, when applying braking method A (left) and braking method b (right) 25

Figure 10: Chemical composition of the brake pad from Metro Lisbon..... 26

Figure 11: Line map of the Metro in Sofia; the relevant Metro line M1 is marked with a red ellipse and demo station Opalchenska with a black ellipse (source: <https://www.metrosofia.com/en/maps#pid=1>) 27

Figure 12: Development of the friction surface over the run-in process of in total approx. 2000 brake applications..... 28

Figure 13: Velocity of the metro and the average wheel temperature (3 measuring positions) during a driving cycle with maximum (red) and minimum load (blue) for braking method A .. 29

Figure 14: velocity of the metro and average wheel temperature (measured with 3 sliding thermocouples) for braking method B at maximum load operation 30

Figure 15: Friction coefficients of the block brake from Sofia for braking method A and B at maximum load..... 31

Figure 16: Particle number concentration over the respective test cycle of the brake types used in the metros..... 32

Figure 17: Average brake particle size distribution for braking method A in maximum load operation (red) and minimum load operation (blue) 33

Figure 18: Mass-related composition of PM₁₀ brake dust for braking method A in maximum load operation (left) and minimum load operation (right)..... 34

Figure 19: Mass-related composition of PM_{2.5} brake dust for braking method A in maximum load operation (left) and minimum load operation (right)..... 35

Figure 20: Mass-related composition of the brake sole material 35



LIST OF ABBREVIATIONS

ACRONYM	DESCRIPTION
AES	Atomic emission spectroscopy
Ba	Chemical symbol for barium
CPC	Condensation Particle Counter
EC	Elemental Carbon
D	Deliverable
Fe	Chemical symbol for iron
FID	Flame Ionisation Detector
FMPS	Fast Mobility Particle Sizer
GC	Gas chromatography
GTR	Global Technical Regulation (here referring to UN GTR No. 24: Laboratory Measurement of Brake Emissions for Light-Duty Vehicles)
HEPA	High Efficiency Particulate Air (Filter)
HF	Hydrofluoric acid
ICP	Inductively coupled plasma
IUTA	Institut für Umwelt & Energie, Technik & Analytik e. V. (AeroSolfid partner)
LC	Liquid chromatography
LOD	Limit of detection
LOQ	Limit of quantification
LVS	Low Volume Sampler
MS	Mass spectrometry

OC	Organic carbon
OPS	Optical Particle Sizer
PM	Particulate Matter
PM _{2.5}	Particulate matter suspended in air which is small enough to pass through a size-selective inlet with a 50 % efficiency cut-off at 2.5 µm aerodynamic diameter (From EN12341-2023)
PM ₁₀	particulate matter suspended in air which is small enough to pass through a size-selective inlet with a 50 % efficiency cut-off at 10 µm aerodynamic diameter (From EN12341-2023)
Sb	Chemical symbol for antimony
TÜV	Technischer Überwachungsverein (operator of dynamometer test rig; subcontractor of IUTA)
UFP	Ultrafine particles, i.e. particles with sizes below 100 nm (0.1 µm)
WP	Work Package

LIST OF SYMBOLS

SYMBOL	DESCRIPTION
d_p	Particle diameter [nm]
m	Mass [kg]
N	Particle number concentration [$1/\text{cm}^3$]
z	Charge [As]
μ	Friction coefficient [-]

PUBLISHABLE SUMMARY

Emission of brake dust has raised increased awareness over the last years due to its potential toxicity. The Euro 7 legislation will for the first time set limit values for brake dust emission factors of road vehicles. In contrast, no such approaches have been made to lower the dust emissions from brakes used in rail vehicles. In the case of underground trains, such as municipal metro lines, these emissions can be particularly harmful for passengers and workforce, because the concentrations can accumulate over time in the often poorly ventilated tunnels. One goal of the AeroSolfd project is therefore to reduce the exposure of humans in metro stations to train-generated brake dust by improving air quality locally with the help of air cleaners. The efficacy of the air cleaners shall be demonstrated at two metro stations, one in Lisbon, Portugal (*Alto dos Moinhos* station on the blue line), while only the health impact of brake dust particulate matter will be investigated in Sofia, Bulgaria (*Opalchenska* station on line M1).

Since the air cleaners do not selectively filter brake dust, but also any other particles present in the air, it is necessary to fully characterise the dust emitted by the brakes, in order to be able to determine the air cleaner efficacy for reducing exposure to brake dust only. Ideally, such characterisation yields a physical and/or chemical tracer that is unique for the dust emitted by the brake, so that a reduction of its concentration at the station can be used as a proxy for brake dust reduction. For the characterisation, the emissions from the exact same brakes as used by the metro lines in Lisbon and Sofia, respectively, have been investigated on a dynamometer test bench in two separate measurement campaigns. The trains in the two cities use different brake concepts. Whereas the trains from Lisbon use disc brakes, the trains from Sofia employ block brakes. By choosing the metros from these two cities it was thus possible to cover the two dominant brake technologies for rail vehicles. An open dust sampling system has been developed that allows for collecting the cooling air including the emitted brake dust particles below the brake in the dynamometer test bench. Samples of the aerosol were taken isokinetically and the total number concentration (>10 nm) and number size distribution (5.6 nm – 10 µm) measured. Additionally, particles were collected onto filters downstream of a PM_{2.5} and a PM₁₀ pre-separator for subsequent chemical analyses.

The results of the measurements show that the dust emitted by the two different brakes exhibit very similar number size distributions, with a stable primary mode at around 180 nm (Sofia) and 200 nm (Lisbon) and a secondary peak at around 2 µm. These modal particle sizes can be used as physical tracers for the emissions, as particles of these sizes are not highly abundant in the atmosphere. However, the concentrations, emitted by the two different brakes, were quite different. The block brake from Sofia generated significantly fewer particles than the disc brake from Lisbon. It was further found that the emitted concentrations of ultrafine particles with sizes below 100 nm was highly variable, due to the constantly changing brake temperatures. Ultrafine particles are therefore not useable as a physical tracer, not least because they are ubiquitously present in the atmospheric air.

The chemical composition emitted by the two different brakes was very different and reflected the composition of the brake pad (Lisbon) and brake sole (Sofia), respectively. The PM as well as the pad from Lisbon included antimony (Sb), which had also been used for brakes in road-vehicles but was banned many years ago. Since antimony is not used in other applications and is thus virtually non-existent in the atmosphere, it can be used as a nearly ideal chemical tracer to quantify the amounts of train-generated brake dust at the station in Lisbon. The dust and brake sole from Sofia did not contain antimony, but significant amounts of barium (Ba). Barium is otherwise only used on a small scale, e.g.

as barium sulphate in contrast agents or barium ferrite in magnetic tapes, from where it is very unlikely that it may become airborne. It is therefore suggested to use barium as the chemical tracer for brake dust at the station in Sofia. It may, however, be necessary to use not only the concentrations of Sb and Ba, respectively, but the ratio of their concentrations to the iron (Fe) concentration in the air. Such ratios are reported in the scientific literature to be a better source indicator than the concentration of individual tracer elements. In summary, the laboratory investigations revealed significant differences of the dust released by the two different brake concepts that may lead to different exposures of passengers and workforce. The determined distinct physical and chemical tracers for the two brakes will help to quantify exposure to brake dust only as well as the potential for its reduction by means of air cleaners at the *Alto dos Moinhos* and *Opalchenska* station, respectively.

1. INTRODUCTION

It has been demonstrated in a multitude of studies that airborne particulate matter (PM) can cause adverse health effects [1, 2, 3]. Road traffic is considered a major source of particulate matter in urban environments [4]. However, the share of exhaust emissions has continued to decline over the years due to engine improvements and the introduction of exhaust after-treatment methods. In contrast, particulate emissions due to abrasion from brakes, tyres, and the road surface, as well as due to resuspension have steadily increased [5, 6]. The reason for this, in addition to increasing traffic, is primarily the steadily growing average vehicle size and mass. Whereas a strong focus has, in recent years, been put on the reduction of particulate emissions from road traffic, efforts to reduce the emissions from rail traffic are still rather at an infant stage. WP3 of the AeroSolfd project aims among others at reducing the human exposure at metro stations particularly to brake dust emitted by the train brakes.

While the monitoring of particulate matter concentrations in outdoor air is prescribed by the European Union in the Air Quality Directive 2008/50/EC and corresponding legally binding limit values for PM_{2.5} and PM₁₀ have been issued, the air quality in tunnels and stations of subways is a legal grey area. Limit values exist here only as general occupational exposure limit values and apply only to the employees working there. Due to the (semi-) closed environment of a subway with often only little air exchange, air pollutants such as particulate matter can accumulate over time. Increased concentrations of particulate matter compared to outside air have already been detected in many measurements in subways [7, 8, 9]. Based on the chemical composition of particles found at subway stations [10], it can be concluded that train brakes are a major source of particulate matter in subway tunnels. Extensive studies of brake dust emissions have already been carried out for road vehicles [11, 12], which have shown, among other findings, that the sizes of the emitted particles depend strongly on the brake temperature [13, 14, 15]. At low temperatures particles are essentially formed mechanically by abrasion, whereas very small particles are newly formed by nucleation at elevated brake temperatures. In this case, brake pad material evaporates and supersaturates as the air cools down, leading to the formation of molecular clusters that eventually reach the size of particles. Nucleation causes the formation of very small particles with sizes in the single-digit nanometre range at very high number but only very low mass concentrations. A standardisable test set-up has been developed and published for these measurements of the emissions from passenger car brakes on a dynamometer test rig. With this set up, particle mass-based [16] as well as the number-based [17] emission factors can be determined reproducibly, based on a specified test cycle [18]. This setup provides for the brake to be completely enclosed on a brake dynamometer test bench and for clean (cooling) air to flow through the enclosure. Downstream of the enclosure, aerosol samples are continuously taken from the total flow and fed to the measuring instruments.

While approaches to reduce brake dust emissions for car brakes already exist based on filter solutions [19, 20], exposure to brake dust in metro stations has not yet been the focus of public attention. The AeroSolfd project tackles this challenge by installing air purifiers (Filter Squares) at demo sites like metro station *Alto dos Moinhos* in Lisbon. The air purifiers will thus help to reduce the exposure of passengers and employees to harmful brake dust. However, the air cleaners do not exclusively filter brake dust, but also particulate matter from other sources. On the one hand, this is certainly positive, because it reduces the total exposure of people at a metro station. On the other hand, it makes the quantification of the efficacy of the air cleaners for brake dust more complex.

A differentiation between brake dust and other ubiquitous ambient particles can be achieved, if characteristic tracers for particulate matter emitted from metro brakes can be identified. For the

determination of the tracers, measurements were carried out at a dynamometer test rig with a clean background environment. The measurements were conducted using the exact same brakes as used by metro Lisbon and metro Sofia, respectively. The two brakes follow different brake concepts, i.e. disc brake in the case of Metro Lisbon and block brake in the case of Metro Sofia. The brakes along with the necessary documentation, e.g. on the profile of the corresponding metro lines, were supplied by the corresponding project partners. This report describes the measurement set up including the sampling system and measurement equipment, the measurements carried out on both brakes along with the data analysis and eventually presents the derived physical and chemical tracers for the dust emitted by the two brakes and draws conclusions.

1.1.PURPOSE AND TARGET GROUP

The primary purpose of D3.1 is to characterize typical particle sizes and chemical composition of PM_{2.5} and PM₁₀ particles emitted by the brakes used by the metros in Lisbon and Sofia. The typical sizes shall be used as physical tracers and typical chemical composition as chemical tracers for brake dust exposure at metro stations in the two cities. One metro station in each of the two cities has been identified as demo sites for the determination of the efficacy of Filter Squares to reduce the exposure of passengers and staff to brake dust at the metro station in task 3.2, i.e. *Alto dos Moinhos* on the Blue Line in Lisbon and *Opalchenska* on the line M1 in Sofia. For this purpose, the concentrations of the physical and/or chemical tracers measured at the two stations shall ideally unambiguously stem solely from the emission of brake dust.

The main target group for the results in this deliverable report are consequently the partners involved in the exposure measurements at the metro stations in task 3.2. However, it is expected that the results are also of interest for a larger audience both in academia as well as in the area of metro or train operators. It is therefore intended to publish the results in dedicated scientific full open access journals.

1.2.CONTRIBUTIONS OF PARTNERS

Table 1. Contribution of each partner in this deliverable

PARTNER SHORT NAME	CONTRIBUTIONS
IUTA	Lead the deliverable; designed and constructed the sampling setup; carried out the measurements at a dynamometer test rig; data evaluation
Metro Lisbon	Provided brake and information on profile and braking strategy
Metro Sofia	Provided brake and information on profile and braking strategy
CSIC	Contribute to the measurements at a dynamometer test rig; data evaluation

2. OBJECTIVES AND EXPECTED IMPACT

The overall goal of WP3 is to develop a blueprint aimed at significantly reducing air pollution in public transport-related semi-enclosed micro-environments by using enhanced air purifier designs and innovative brake dust retrofit solutions.

2.1.OBJECTIVES OF D3.1

Task 3.1 has the following specific objectives:

1. Characterise the dust emissions of a brake, used by Metro Lisbon on the Blue Line in terms of the number size distribution and the chemical composition on a dynamometer test rig using a typical driving/braking pattern for this line.
2. Characterise the dust emissions of a brake, used by metro Sofia on the line M1 in terms of the number size distribution and the chemical composition on a dynamometer test rig using a typical driving/braking pattern for this line.
3. Determine one or more typical particle sizes (physical tracer) and one or more typical chemical compounds or specific ratios of chemical compounds (chemical tracer) emitted by each of the brakes, that is/are otherwise not or at least not highly abundant in air.
4. Estimate the contribution of brake emissions to air and water quality and damage to historic buildings.

2.2.EXPECTED IMPACT

Brake dust is known to be a main contributor to often rather low air quality in metro tunnels and stations. Thus far, relatively little is known about the properties of brake dust from metro brakes and the exposure of passengers and staff to these particles. One major goal of WP3 is to reduce the exposure of humans to brake dust particles in metro stations by the use of air purifiers. The chemical and physical tracers derived in task 3.1 for the exact same brakes as used by two partners operating the metro in Lisbon and Sofia are key to quantify the exposure with and without air purifier operation at the two demo sites. Only with the help of these tracers, it will be possible to quantify the efficacy of the air purifiers at the two demo sites in T3.4 and T3.5. With this knowledge, the air purifiers or their operation can be optimised, eventually leading to an increased credibility of the Filter Squares as a commercial product or service.



3. DESCRIPTION OF TECHNICAL/SCIENTIFIC ACTIVITIES

None of the project partners owns a dynamometer test rig that can be used to carry out measurements on tram, metro, or train brakes. Consequently, and in accordance with the DOA, IUTA first published a call for tender for a subcontract that covers the rent and operation of a suitable dynamometer test rig. The most economically feasible offer was provided by TÜV Nord in Essen, who were thus subcontracted by IUTA.

3.1.DEVELOPMENT OF A SAMPLING SYSTEM FOR CHARACTERIZING DUST EMISSIONS OF METRO BRAKES ON A DYNAMOMETER TEST RIG

Firstly, an appropriate dust sampling system for the dynamometer at TÜV Nord needed to be designed and built. In contrast to the GTR-design for the sampling system for light-duty vehicles, an open sampling system was favoured here over a full enclosure of the brake. Unlike in the case of measurements in accordance with the GTR, it is not the aim of the measurements carried out here to determine quantitative emission factors for the brake, i.e. the total mass or number of particles emitted per kilometre. Instead, the aim is to identify typical particle sizes and typical chemical compositions of the emitted dust. For this, an enclosure that assures all emitted particles to be carried away by the cooling airflow, but that would be very difficult to implement in the TÜV test rig, is not required.

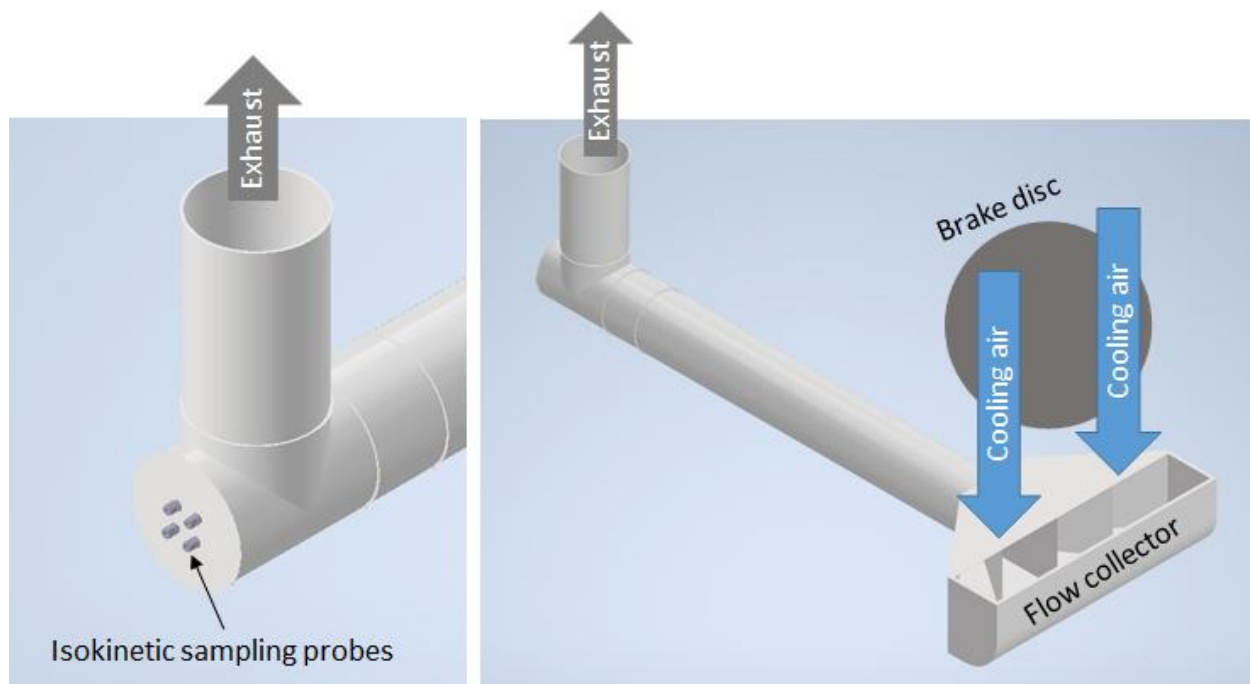


Figure 1: 3D CAD drawings of the sampling system for the measurement of dust emitted from metro brakes

In the dynamometer test rig of TÜV Nord, the cooling air for the brake enters the space above the brake through a rectangular outlet approximately 1 m above the brake. From there, the air flows straight down and is collected again in a flexible air outlet. The brake assembly is located inside a chamber, which is completely closed during each brake test. For the measurements, carried out in

WP3.1, the cooling air supply was equipped with a HEPA H13 filter to assure high cleanliness of the incoming air and consequently low background concentration inside the closed chamber. 3D CAD drawings of the sampling system, designed for the measurements are shown in Figure 1. The system has been constructed from stainless steel and consists of a rectangular flow collector that is placed underneath the brake assembly and collects the top-down cooling air flow as shown in Figure 2. After a 90° bend, the air is carried away inside a 150 mm diameter circular tube. After a distance for flow homogenisation, up to four isokinetic probes are installed that can be connected to the aerosol measurement and sampling equipment. The outlet of the tubing downstream of a 90° elbow is connected to the ventilation system of the dynamometer test rig that recirculates the cooling air.

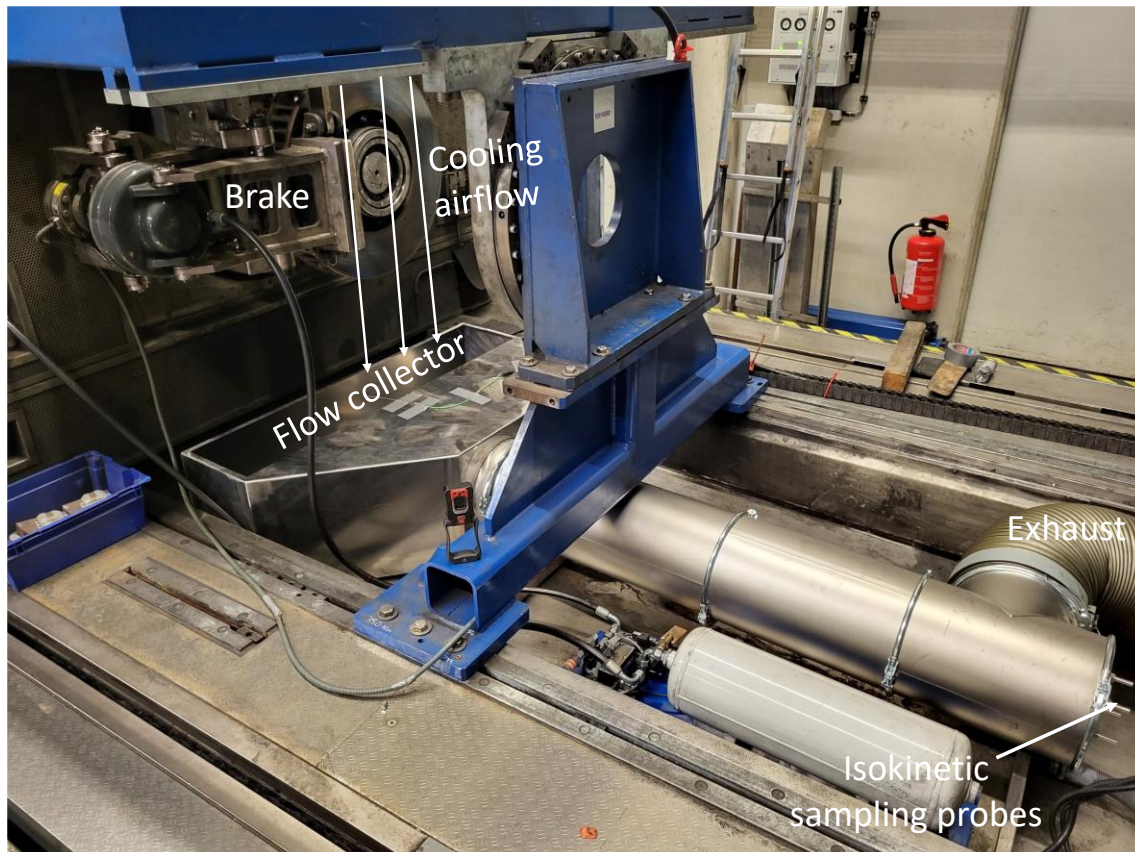


Figure 2: Photograph of the installed sampling system

3.2. MEASUREMENT EQUIPMENT

In order to determine typical particle sizes and typical chemical compounds of the dust emitted by the brakes, it is necessary to include both direct-reading, size-resolving measurement equipment to determine the physical tracers as well as samplers to collect the particles for subsequent analyses for the chemical tracers. From measurements on passenger car brakes it was expected that a wide range of particle sizes are emitted. In the case of car brakes, they include a very small (<20 nm) fraction that is formed by evaporation of pad material when the brake gets hot followed by new particle formation due to nucleation upon cooling. A medium sized fraction (~0.2 μm) and a fraction of larger (~2 μm) particles are formed by mechanical processes, i.e. abrasion [13].

3.2.1. DIRECT READING MEASUREMENT EQUIPMENT

A combination of two measurement devices was employed to cover the full-size range, i.e. a Fast Mobility Particle Sizer (FMPS, TSI model 3091) and an Optical Particle Sizer (OPS, TSI model 3330). The FMPS measures the number size distribution of airborne particles in a size range from 5.6 nm to 560 nm (0.0056 – 0.56 μm) with a time resolution of 1 s. In the FMPS, the incoming particles are initially charged in a unipolar charger to obtain a defined size-dependent charge distribution. The particles are then classified according to their electrical mobility into 22 mobility classes. The electrical mobility is essentially the ratio of the particle charge and the size. The current stemming from each mobility class is measured by sensitive electrometers as a measure for the particle concentration in this mobility class. A complex data deconvolution algorithm is internally applied to obtain the number size distribution with a resolution of 16 size channels per decade. The total aerosol flow rate drawn by the FMPS is 10 l/min.

The OPS measures the number size distribution of airborne particles also with 1 s time resolution in a size range from 0.3 μm to 10 μm (300 – 10,000 nm), based on the measurement of the intensity of light scattered by individual particles. The resulting number size distributions are provided with a size resolution of 16 size classes. The flow rate of the OPS is 1 l/min.

In addition to FMPS and OPS, a Condensation Particle Counter (CPC, TSI model 3950) was used to measure the total number concentration of particles larger than 10 nm (0.01 μm). The CPC draws in the aerosol at a flow rate of 1 l/min and exposes the particles to an atmosphere, supersaturated with butanol vapour. As a consequence of the supersaturation, the vapour condenses onto the particles and lets them grow to droplets with sizes in the micrometre range, which are large enough to be counted optically. Unlike the FMPS, a CPC is thus a true particle counter. The CPC was freshly calibrated and was thus used as a quasi-reference for the total number concentration. It was mainly applied to verify the proper operation of the FMPS.

3.2.2. FILTER SAMPLERS

Two low volume samplers (LVS 3.1, Comde Derenda) were used to collect particles onto 47 mm diameter quartz-fibre filters for subsequent gravimetric and chemical analysis. One sampler was equipped with a PM_{2.5} and the other with a PM₁₀ impactor upstream of the filter. Both samplers drew an airflow of 2.3 m³/h each. The samplers as well as the filter handling were fully compliant with EN12341 [21].

Quartz fibre filters were preferred in this study over Teflon-coated filters, since they can be chemically analysed more easily and accurately with lower limit of detection (LOD) and limit of quantification (LOQ). To determine the chemical composition of the particles, initially, a small piece of the filter was punched out and analysed for the content of organic (OC) and elemental carbon (EC) using a thermo-optical analyser (EC/OC analyser, Sunset Laboratories). In this instrument, the filter chunk is exposed to a temperature profile initially under a pure helium atmosphere and later a helium-oxygen atmosphere. During exposure to the He-atmosphere, the organic carbon evaporates as methane and is detected by means of a flame ionization detector (FID). When oxygen is added to the atmosphere, the elemental carbon is emitted as CO₂, which then reacts with added hydrogen to methane, which again is detected by the FID.

The composition of the dust on the remaining filter pieces was first transferred into a liquid. For this purpose, a microwave-assisted chemical digestion was used. The quartz filters were chemically

digested in a mixture of nitric acid (HNO₃) and hydrofluoric acid (HF). Chemical digestion converts solid elements from insoluble substances into soluble ionic species. This acid combination is suitable for a wide range of inorganic quantitation requirements, as HNO₃ oxidises most inorganic substances and converts them into water-soluble nitrate salts. The addition of HF ensured complete digestion of silicates and some oxides that may occur and prevents the inclusion of analytes in insoluble particles. Digestion was performed at 180 °C for 60 minutes to obtain a clear solution. A microwave (model MARS 6, CEM) was used for this purpose. Since many elements were present only in traces, the resulting solutions were concentrated by evaporation. This step also allowed the removal of hydrofluoric acid to ensure safer handling but also material compatibility during subsequent analysis. Evaporation had no effect on the element amounts, which have much higher boiling points compared to water and the acids used.

The subsequent element quantification of the liquid samples was done by means of inductively coupled plasma (ICP) systems with atomic emission spectroscopy (ICP-AES, model iCap-6500, Thermo Fisher Scientific) and mass spectrometry (ICP-MS, model iCap-Q, Thermo Scientific). Both systems first nebulise the liquids to be analysed into the plasma source for simultaneous atomisation, ionisation and excitation of the sample components. The plasma formed is based on an argon stream, which is kept in an active state by a subsequent induction force. Temperatures are in the range of 6,000 K to 10,000 K.

ICP-AES exploits the emission of light from the relaxation of excited ionic species formed by thermal excitation. The emitted wavelengths are characteristic for each element and allow quantification by external calibration. The operating range for most elements in ICP-AES is in the range of 0.1 to 10 mg/l.

ICP-MS separates ionic species by mass spectrometry, which is also used in GC-MS and LC-MS techniques. Ions are distinguished by mass-to-charge ratio (m/z) and finally detected with secondary electron detectors, which generate current by discharging the colliding ions. The measuring ranges of such systems are lower by a factor of 1,000 than with ICP-AES, i.e. the measuring ranges start at about 0.1 µg/l for most elements.

3.3. MEASUREMENTS CARRIED OUT ON BRAKE FROM METRO LISBON

3.3.1. MEASUREMENT PROTOCOL

The first AeroSolfid demo site, in which the efficacy of the air cleaners will be demonstrated is the *Alto dos Moinhos* metro station of the Blue Line in Lisbon (see Figure 3).

In preparation for the measurements, the partner Metro Lisbon sent the necessary documentation on the line profile to program the dynamometer test rig. The driving cycle in the measurement protocol includes the entire route of the blue line, including the variable driving speed, acceleration and deceleration, the topography (incline/decline), distances between stations etc. According to the protocol, upon leaving a station, a train quickly accelerates to its cruising velocity of 72 km/h until it approaches the next station and decelerates to a full stop. Besides the documentation, Metro Lisbon also shipped a brake from its stock. The brake tested is therefore the original brake that is used by the trains on the blue line. The trains of Metro Lisbon use disc brakes, similar to common brakes used, e.g., in passenger cars, but larger.



Figure 3: Line map of the metro in Lisbon; the relevant blue line is marked with a blue ellipse and the demo site Alto dos Moinhos with a red ellipse (Source: <https://www.metrolisboa.pt/en/travel/diagrams-and-maps/>)

The original test protocol foresaw that deceleration of the train is generally accomplished 45.1% by friction braking and 54.9% by the use of the recuperation brake, as described in the documentation received from Lisbon. While the measurements were already conducted, a contact at Metro Lisbon mentioned in a video conference that this ratio is not realistic, because modern trains would mainly use the recuperation brake to slow down the train and apply the friction brake only to come to a full stop. A second braking method was therefore also tested in which only the recuperation brake is used to slow down from 72 km/h to 10 km/h. Only for velocities below 10 km/h and to come to a full stop, the friction brake is additionally applied in this concept in the same ratio (45.1%/54.9%) as mentioned above. In the following, braking method A refers to the concept in which 45.1% of the braking energy is taken up by the friction brake and 54.9% by the recuperation brake throughout the deceleration. Method B refers to the concept in which at velocities >10 km/h, only the recuperation brake is applied and the same ratio of recuperation to friction brake at velocities below 10 km/h.

3.3.2. RESULTS FROM METRO LISBON

3.3.2.1. DRIVING CYCLE AND RESULTING BRAKE TEMPERATURES

Figure 4 shows the driving cycle for a complete roundtrip of a blue line metro train along with the necessary friction coefficients and resulting brake disc temperatures using method A.

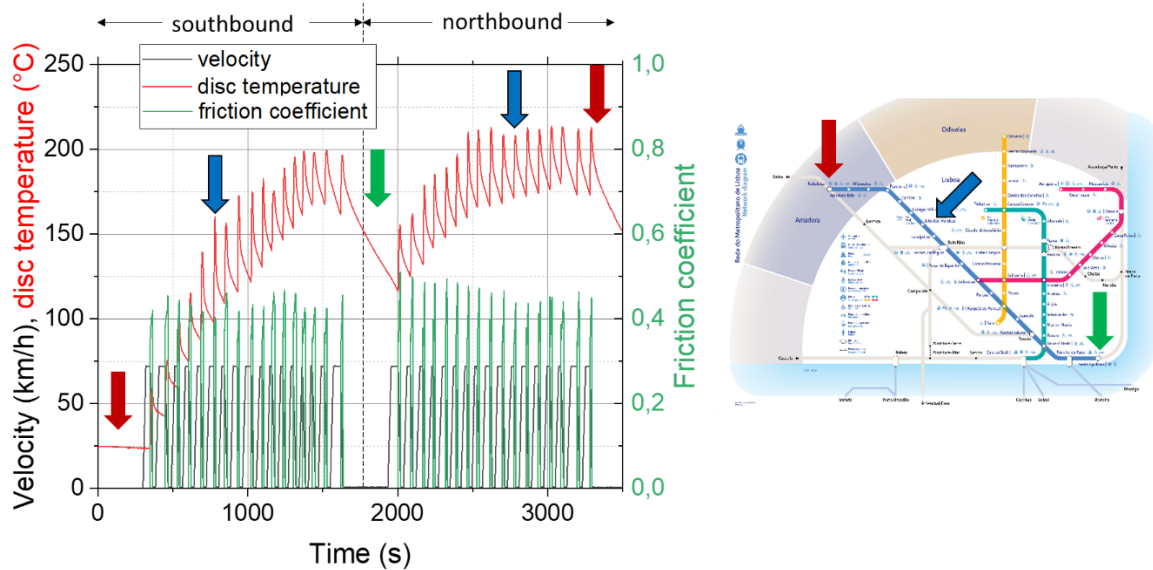


Figure 4: Driving speed (black), brake disc temperature (red) and friction coefficient (green) during a full return trip of the blue line using braking method A; first/last station Reboleira (red arrow), demo site Alto dos Moinhos (blue arrow), turnaround station Santa Apolonia (green arrow)

The results shown in the figure are from the first measurement carried out with this cycle, mimicking the first roundtrip of a train on a day. Consequently, the brake disc temperature is initially at room temperature and then increases, every time the friction brake is operated. The cooling air temperature was approximately 25°C, which represents a typical air temperature in a metro during summer months. Between two brake events, the disc temperature cools down. It can be seen that the disc temperatures reach values, which for passenger cars have been identified as above the critical temperature levels (160-180°C) for the onset of new particle formation by nucleation. However, during the measurements carried out here, the formation of nucleation particles has in some cases already been observed at lower temperature levels. A possible reason may be that the disc temperature is probably not as good an indicator for the (more relevant) brake pad temperature as in the smaller car brakes, due to the much higher heat capacity of the train brake discs.

Upon arrival at the final destination of the southbound trip, the start of the northbound trip commenced after a wait time of 5 minutes during which the brake cooled further down. However, the eventual temperature before the departure of the train was still above room temperature. Like during the southbound trip, the disc temperature again increased with each braking event, but reached a reproducible temperature cycle after the seventh station. The same behaviour was seen for each individual measurement, i.e. the disc temperature peaked at around 210° during each braking event and then dropped to around 175°C during the movement of the brake.

Figure 5 shows the driving speed, friction coefficient μ and resulting brake disc temperature obtained applying braking method B. It can be seen from the curve of the friction coefficient that the duration of the use of the friction brake is much shorter than when using method A, because the friction brake is only used to bring the train to a complete stop. As a result, a lot less kinetic energy is absorbed by the friction brake, causing the disc temperature to be almost unaffected by the braking events and to remain nearly constant, close to the cooling air temperature. As a result of this temperature profile, it can be concluded that new particle formation due to nucleation is not expected to occur with method B.

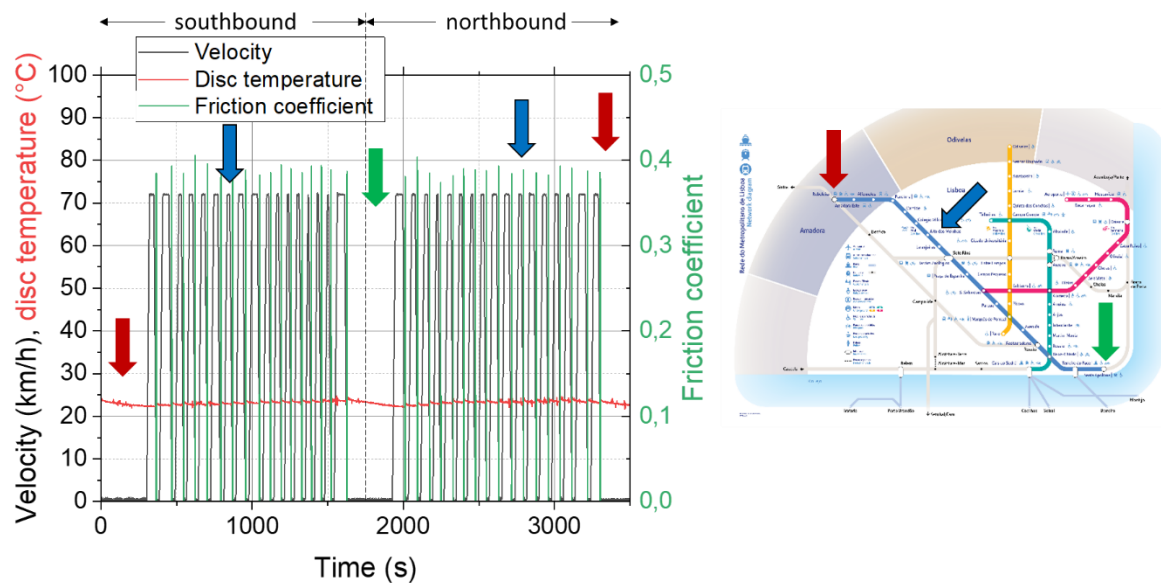


Figure 5: Driving speed (black), brake disc temperature (red) and friction coefficient (green) during a full round trip of the blue line using braking method B; first/last station Reboleira (red arrow), demo site Alto dos Moinhos (blue arrow), turnaround station Santa Apolonia (green arrow)

3.3.2.2. RESULTS FROM PHYSICAL AEROSOL CHARACTERISATION

A detailed analysis of the particle number size distributions measured with the FMPS and OPS was carried out by comparing the results from each individual braking event. It was found that the size distributions did not systematically differ from station to station. However, the brake disc temperature did have an effect on the number size distribution in the ultrafine ($<0.1 \mu\text{m}$) particle size range, due to nucleation, which cannot be systematically controlled. Measurements were further carried out for different vehicle weights, assuming an empty train and a train occupied with the maximal allowed and a medium number of passengers. The results showed that the number of passengers only had a small impact on the total concentration, but not on the size distribution of the emitted particles. For the purpose of this study, i.e. identifying typical particle sizes, it was thus concluded that the number of passengers is no variable to be further investigated. All results presented in the following were obtained for a medium number of passengers.

Figure 6 shows the average number size distribution of the brake dust emitted during stops at the 17 stations of the blue line during five round trips using braking method A. The graph shows that the vast majority of the particle number concentration stems from particles is in the submicron particle size range. The results of the FMPS and OPS in the overlapping size range are in reasonably good agreement, considering the very different measurement principles and that both devices deliver particle sizes as different equivalent diameters.

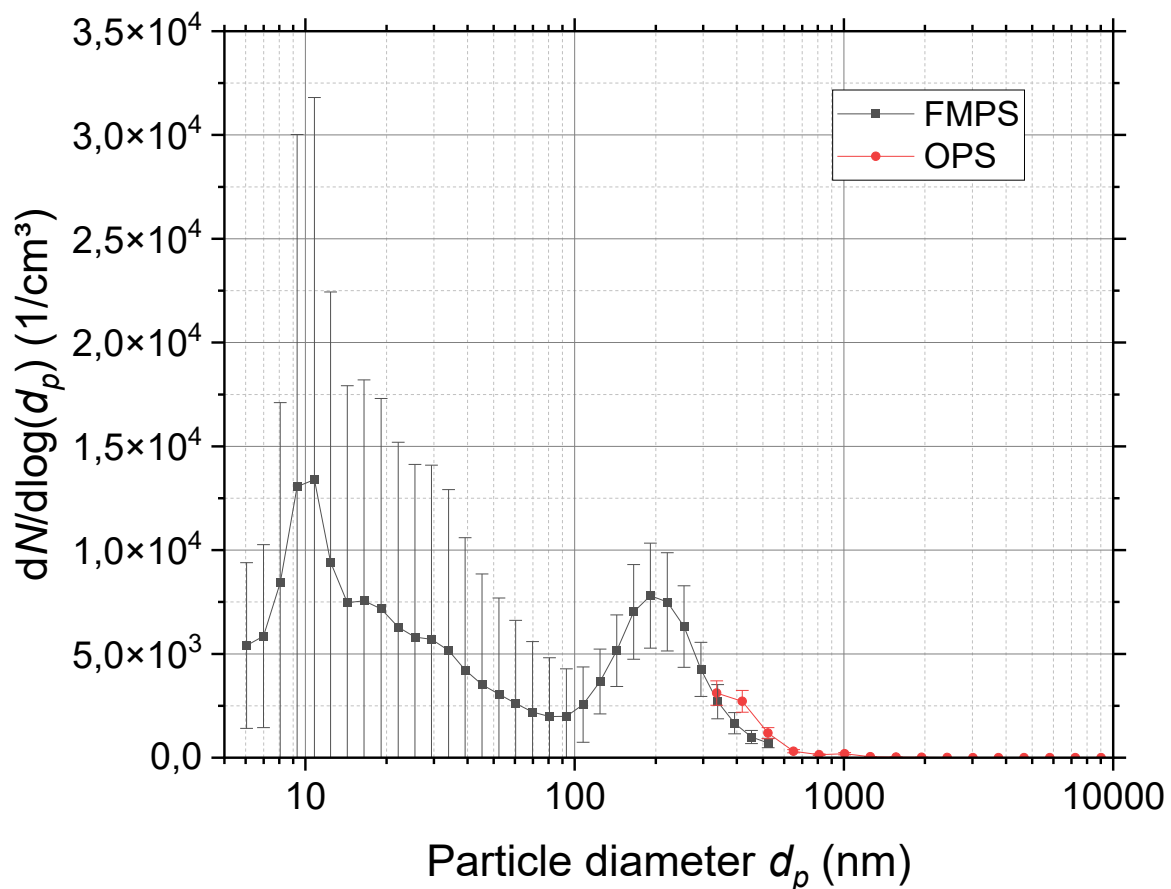


Figure 6: Average number size distribution of brake dust emitted from the brake from Metro Lisbon measured with FMPS and OPS using braking method A; average of all stops at the 17 stations during five round trips; error bars indicate the standard deviations of the concentrations in each particle size class.

The average number size distribution exhibits two distinct modes, one at around 20 nm and the other at 200 nm. The mode at 20 nm mainly comprises particles that are freshly formed by nucleation. These particles were observed during nearly every braking activity, however at highly variable concentrations and sizes (note that the two are connected due to coagulation). As a result of this unsteady particle generation the errors bars in the size classes below 100 nm are rather large.

The second mode at around 200 nm is likely formed by abrasion of brake material. Since this process always occurs, when the brake is applied, the formation of this mode is much more reproducible. Consequently, the error bars are much smaller for concentration of these particles.

The average number size distribution, obtained during the measurement of the stops at each of the 17 stations during a total of 17 round trips applying braking method B is illustrated in Figure 7. It can firstly be noticed that the total number concentration is significantly lower compared with method A (Figure 6). This was expected, because in method B the friction brake is only used to bring the train to a full stop and thus absorbs a lot less energy. It can further be seen that the size distribution in the ultrafine particle (UFP) size range (>100 nm) is different during measurements applying method B compared with method A. Particularly, when considering that the particle background in the measurement system, which could not be completely eliminated despite the use of the HEPA H13 filter due to the not completely sealed chamber. The size distribution of the background particles is added

to Figure 7 as a dotted line. It can be seen that the size distributions in the ultrafine size range in the background and during braking events are nearly identical up to a particle size of approximately 60 nm, whereas the second mode at around 200 nm is clearly much higher.

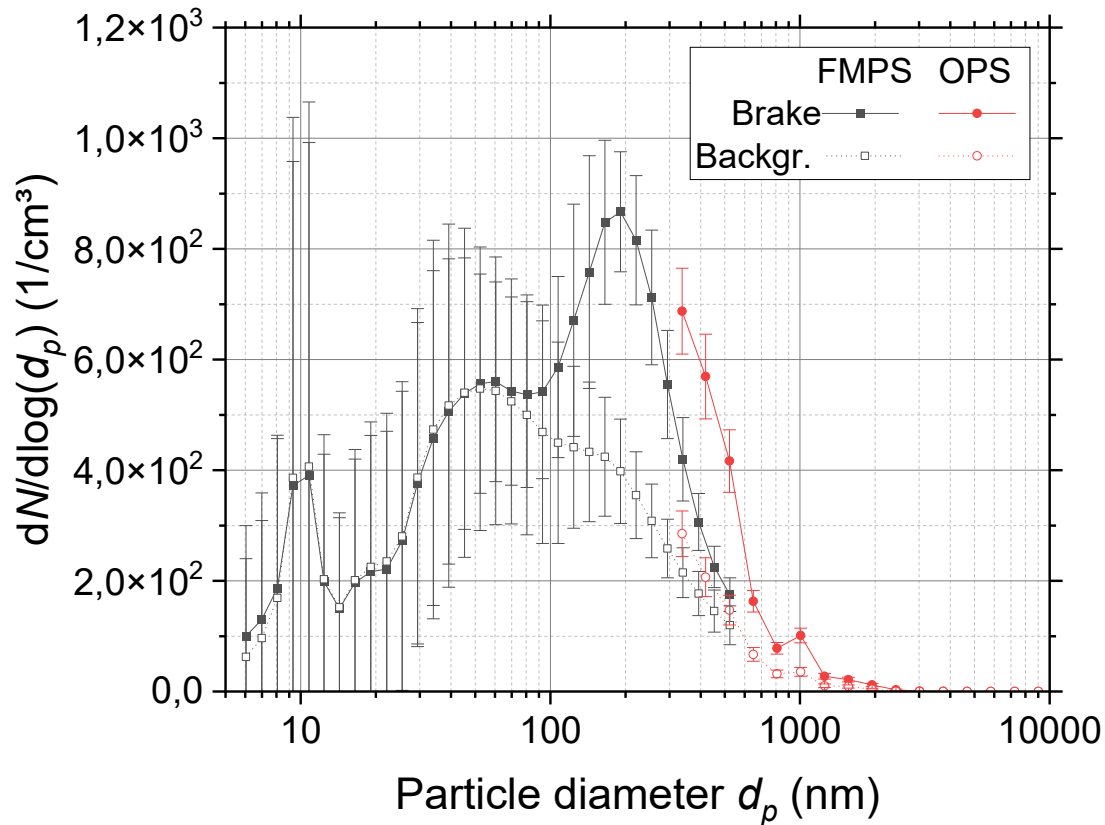


Figure 7: Average number size distribution of brake dust emitted from the brake from Metro Lisbon measured with FMPS and OPS using braking method B; average of all stops at the 17 stations during 17 round trips; error bars indicate the standard deviations of the concentrations in each particle size class

A comparison of the average number size distributions, measured applying method A and B is shown in Figure 8. The background size distribution has been subtracted from both average distributions shown. Note that the concentrations for method A correspond to the primary y-axis, whereas the concentrations for method B refer to the secondary y-axis. For the sake of clarity of the representation, no error bars are presented in this graph.

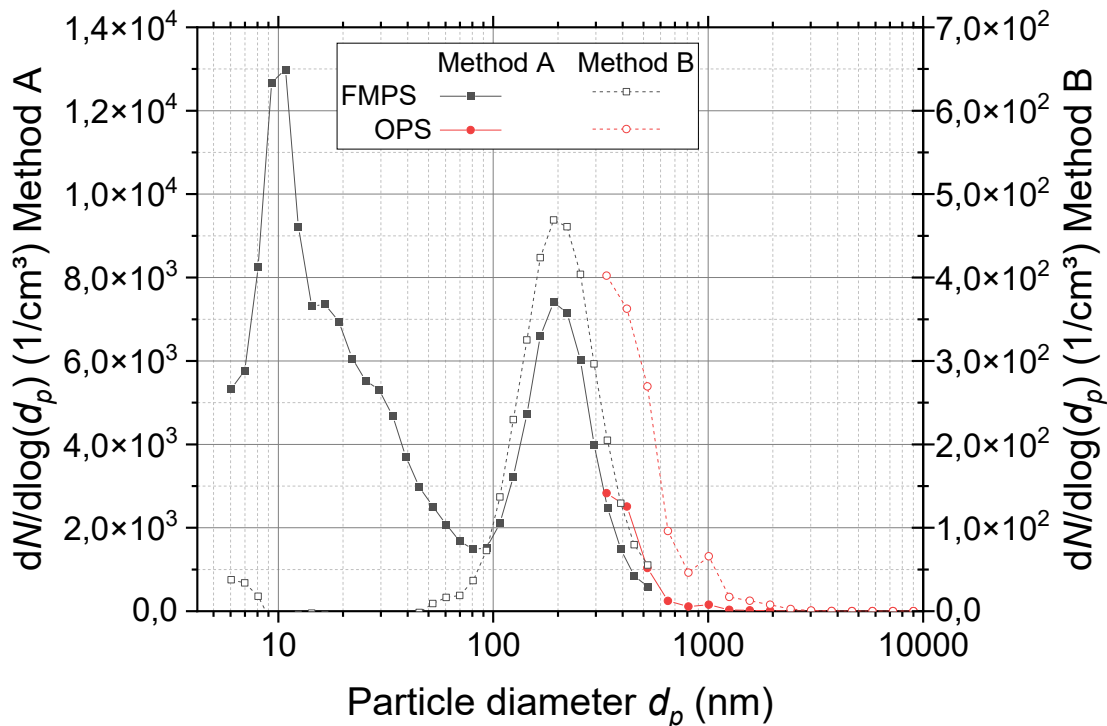


Figure 8: Average particle number size distributions emitted by the brake from Metro Lisbon, measured applying method A (primary concentration axis) and method B (secondary concentration axis); background number size distribution subtracted for both

The graphs in Figure 8 show that the mode at a size of around 200 nm is very similar in terms of the modal diameter and geometric standard deviation (width), although the total number concentration differs by a factor of nearly 30. It should further be noted that particles with sizes of ~200 nm are not highly abundant in the ambient atmosphere. It is consequently suggested to use particles with a (mobility) diameter of 200 nm as the physical tracer for the measurements at the demo site *Alto dos Moinhos*.

3.3.2.3. RESULTS FROM CHEMICAL AEROSOL CHARACTERISATION

The collected filters were first weighed to determine the total mass of collected particles by subtracting the mass of the loaded filters from the mass of the unloaded filters, determined prior to the measurements. The entire procedure was in full compliance with EN 12341 [21]. The masses of the different elements, determined from the filter samples as described in section 3.2.2 were then related to the total gravimetrically determined particle mass.

Figure 9 shows pie-charts for the chemical composition, obtained from the $PM_{2.5}$ filters sampled when applying method A (left) and method B (right). The composition of the collected PM_{10} was generally quite similar and is therefore not explicitly shown here. Only those elements that could be quantified (i.e. their concentrations were above the limit of quantification (LOQ) of the respective analytical technique) are shown in the figure. Those elements with concentrations below the LOQ and those that could not be identified are summarised as “rest”. The pie-charts show that the elements present during both braking methods are generally the same, but the relative abundances differ significantly. Whereas

iron (Fe) is the main element emitted during method A, contributing to 36.3% of the total particle mass, it only amounts to 7.4% during method B. When applying method B, the majority (70.2%) of the total mass is organic carbon. Filter samples taken from the background air, when no brake test was conducted, proved that the OC stems from the background and not the brake. Due to the generally low concentrations emitted during method B (see Figure 8), the background concentration had a non-negligible impact on the composition of the collected particles. Most other elements found, like copper (Cu), nickel (Ni) or chromium (Cr), are rather typical for brake dust, but are also abundant in ambient air. However, the graph also shows that the collected brake dust also contained antimony (Sb). Antimony has been added to brake pads as antimony (III) sulphide acting as a lubricant and has for a long time been used as a tracer for airborne brake wear near roads [22]. Since after its release, antimony can react to form carcinogenic antimony trioxide (Sb_2O_3) [23], Sb has meanwhile been banned from brake materials for road vehicles, but it is still being used for rail vehicles.

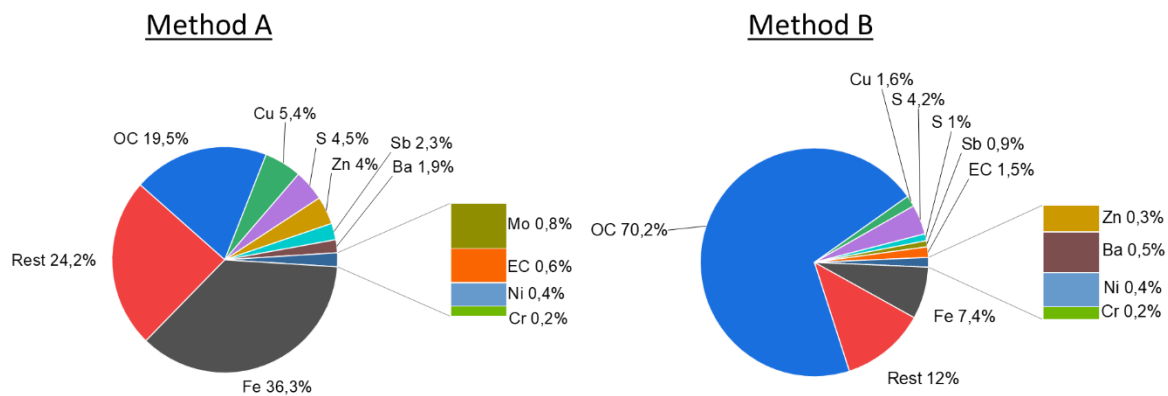


Figure 9: Average composition of $PM_{2.5}$ emitted by the brakes from Metro Lisbon and collected on filters, when applying braking method A (left) and braking method B (right)

In order to ensure that the antimony content measured from the filter samples indeed stems from the brake pads, sample powder was scratched off a pad and chemically analysed. The results shown in Figure 10 confirm the presence of antimony in the brake pad and thus that the measured antimony content stems from the brake pad.

Since it is still used in the brakes from Metro Lisbon and since it is no longer abundant in ambient air, it is suggested to measure the concentration of antimony at the demo site *Alto dos Moinhos* as the chemical tracer to almost unambiguously determine the contribution of the brake dust to the total particle concentration at the station.

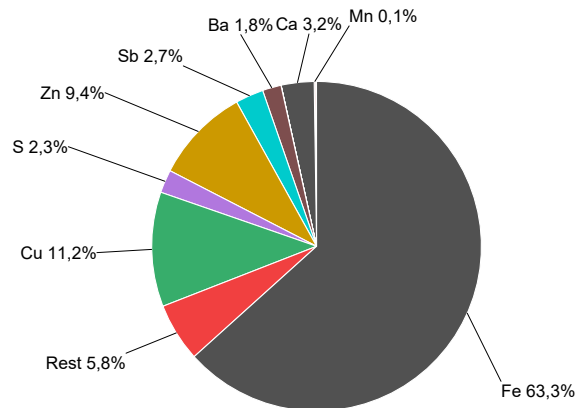


Figure 10: Chemical composition of the brake pad from Metro Lisbon

3.3.3. CONCLUSIONS FROM MEASUREMENTS ON BRAKE FROM METRO LISBON

The results of the measurements show that particles with an electrical mobility diameter of around 200 nm are a reasonable physical tracer. Analysis of the collected filters for their antimony content serves as a unique chemical tracer for particles, emitted by the metro brakes. It is thus recommended to scrutinise the results of the measurements to be carried out at the Alto do Moinhos station in Lisbon for a mode in the number size distribution at around 200 nm and to analyse the sample filters for the antimony content. The ratio of the corresponding concentrations then yields the efficacy of the Filter Squares for brake dust particles at this station.

3.4. MEASUREMENTS CARRIED OUT ON BRAKE FROM METRO SOFIA

3.4.1. MEASUREMENT PROTOCOL

The second demo station, where air purifiers could be tested to reduce exposure to particulate matter is *Opalchenska*, which is part of the M1 metro line in Sofia (see Figure 11). This line uses old trains from Russia. Consequently, spare and wear parts for these trains, including the brake components, are currently sparse due to trade restrictions.



Figure 11: Line map of the Metro in Sofia; the relevant Metro line M1 is marked with a red ellipse and demo station *Opalchenska* with a black ellipse (source: <https://www.metrosofia.com/en/maps#pid=1>)

In comparison to the disc brakes used in Lisbon and described in chapter 3.3, the trains of this line in Sofia are equipped with block brakes. In block brakes, composite brake block soles are pressed onto the running surface of the iron wheels. Due to the current lack of spare parts for the Russian trains, the delivery of the brake components to be tested had to be postponed several times, causing a considerable delay. Eventually, Metro Sofia delivered one complete system, consisting of wheel and brake block, but strictly forbade making any changes to the wheel, because it was still needed as a replacement wheel for the trains afterwards. Since the adaptation of the original wheel to the inertia dynamometer of TÜV Nord would have required drilling holes into the wheel, a comparable wheel from a goods wagon with a slightly smaller running surface radius was used. The original brake block soles, therefore, had to be run in over several hundred braking operations in order to adjust them to the slightly different curvature of the tread of the wheel and thus to ensure a uniform friction surface. A suitable brake calliper was still available at TÜV Nord. The same measurement set up was used as described in chapters 3.1 and 3.2.

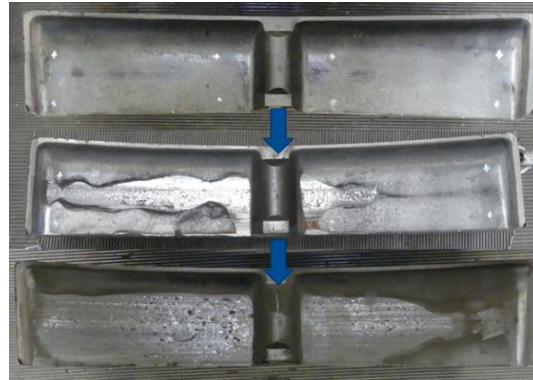


Figure 12: Development of the friction surface over the run-in process of in total approx. 2000 brake applications

Figure 12 shows the development of the friction surface over the entire run-in process with brake applications from initial speeds of 10 km/h to 58 km/h.

By iteratively increasing the initial speed before starting the braking process, it was also possible to estimate the resilience of the brake lining material without any abnormalities in the friction coefficient curve. For reasons of Bulgarian national security, only a single speed-time diagram, covering the *Opalchenska* station and its two neighbouring stations to the north and south, respectively, were provided by metro Sofia. This diagram was used to develop a suitable test protocol for the dynamometer testing. From this diagram, the acceleration, deceleration and constant driving speed could be determined. These values were adopted for the remaining stations, thus neglecting any incline or decline of the track. The lengths of the different track sections, which have a particular effect on brake cooling, were estimated with the help of Google Earth and checked for plausibility against data for this metro line, found on Wikipedia. The evaluation of the documents resulted in a test programme including the 15 underground stations on both the southbound and northbound trip (see Figure 13). The metro accelerates with 1.1 m/s^2 and reaches a constant driving speed of 58 km/h. The deceleration up to a full stop in the underground station occurs at -1.3 m/s^2 . Like in the case for the brakes from Lisbon, two different braking methods were applied. In method A, a combination of the friction brake and electric brake is used during the entire deceleration process, whereas in method B, the friction brake is only applied at velocities below 7 km/h (in Lisbon: 10 km/h) to come to a full stop. In any case, when the friction brake is used, it takes up 23 % of the total brake energy, whereas the electric brake is used for 77 % (information obtained from metro Sofia). For both braking methods two load cases (max. occupancy and empty compartment) were tested and analysed.

3.4.2. RESULTS FROM METRO SOFIA

3.4.2.1. DRIVING CYCLE AND RESULTING BRAKE TEMPERATURES

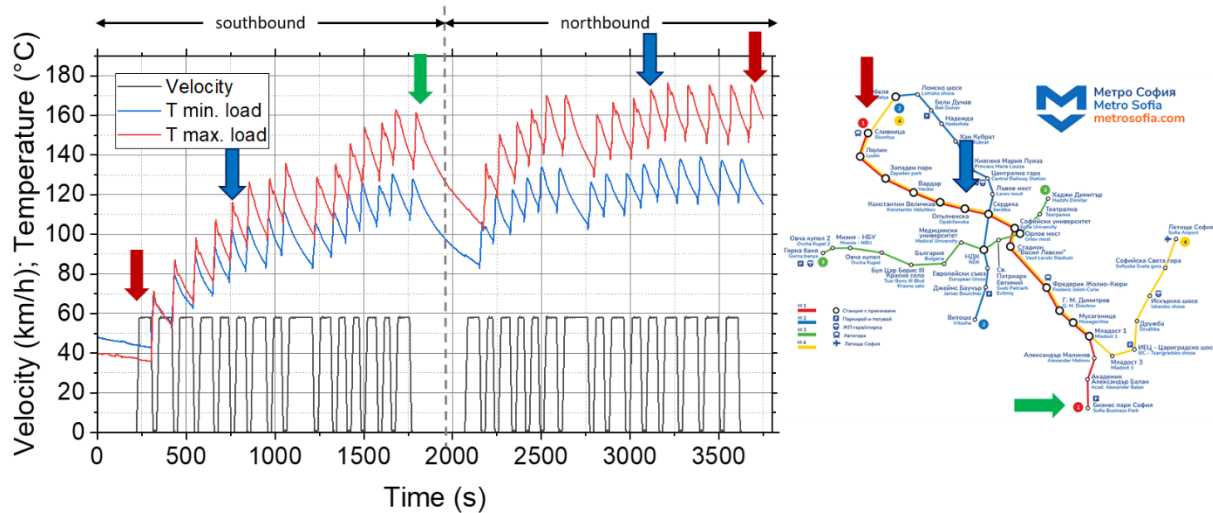


Figure 13: Velocity of the metro and the average wheel temperature (3 measuring positions) during a driving cycle with maximum (red) and minimum load (blue) for braking method A

Figure 13 shows the wheel temperature during the driving cycle in addition to the velocity of the metro. The temperature was measured using six thermocouples, with three measuring points positioned at different distances from the rail guide 5 mm below the running surface; this arrangement of the thermocouples is in accordance with the standard IRS-50548:2022 on the requirements for dynamometer test rigs for the international certification of brakes for rail vehicles. The temperature averaged over the three measuring positions is shown. The maximum temperature difference between the measuring points for braking method A in minimum load operation was 57 °C and 67 °C at full load. A clear difference between the measuring positions was observed for all tests. The measuring position in the centre of the friction surface always showed the highest temperature, while the temperature in the direction of the rail guide was the lowest. A temporal offset and less distinct peaks in the temperature curve were observed during each braking event. It can be assumed that the heat transfer is rather slow due to the high mass of the wheel and that local temperatures vary greatly. The temperature measurement for braking method B with the embedded thermocouples was only partially successful, as the thermocouples sometimes failed to detect a temperature increase for unknown reasons. Sliding thermocouples were therefore also used, which were aligned to the same positions on the running surface as the embedded thermocouples but measured the temperature directly on the surface. This allowed a reproducible temperature curve to be observed, which is why these results are used to visualise the wheel temperature of braking method B. It is shown that less kinetic energy is converted into heat for this braking method. Although the wheel temperature rises briefly by approx. 5 °C, it then drops abruptly to the level of the cooling air temperature (approx. 25 °C).

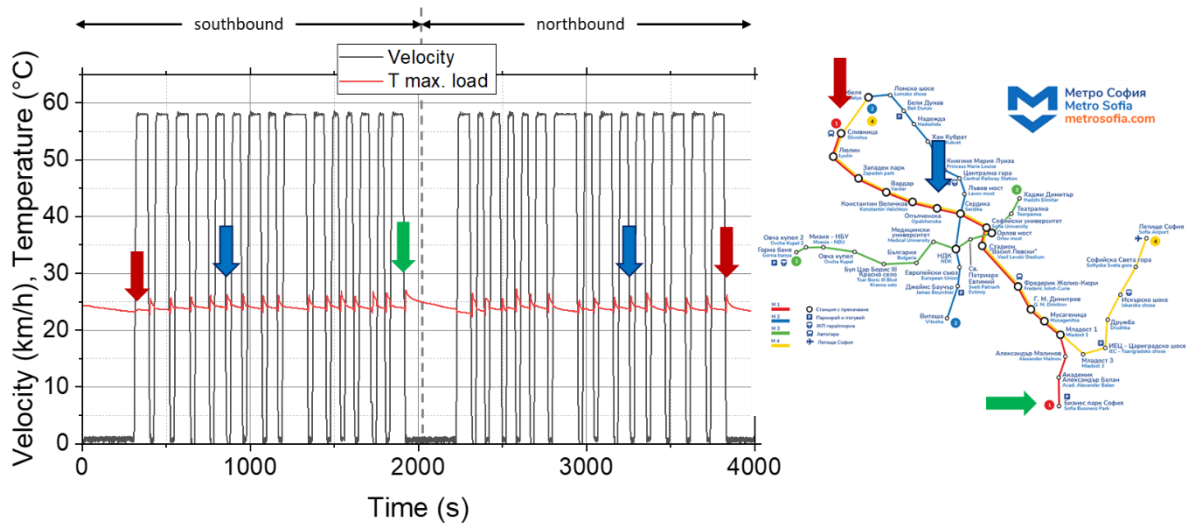


Figure 14: velocity of the metro and average wheel temperature (measured with 3 sliding thermocouples) for braking method B at maximum load operation

The velocity profile and behaviour of the wheel temperature are thus very similar to the results from the tests with the brake from Lisbon, described in chapter 3.3.2. Another important point of investigation is the observation of the coefficient of friction during the driving cycle, particularly because no experience has yet been gained with composite brake block soles. The aim is to ensure that the coefficient of friction remains constant as the brake temperature rises. This prevents brake fading, which can ultimately lead to a loss of braking efficiency due to excessive heat development. The coefficients of friction for braking methods A and B in full-load operation are shown in Figure 15 during one exemplary test cycle.

The increasing temporal offset of the friction coefficient graphs is due to the fact that the purely electrodynamic braking time from 58 km/h to 7 km/h takes around 3 s longer compared to when the block brake is additionally applied. This slight drift means that the braking times of braking method A in this diagram do not perfectly match the braking times of braking method B. The friction coefficient for braking method A shows a slightly stronger scatter in the first half of the southbound trip. This could possibly be due to the still low temperature and simultaneously high braking force. As the temperature rises, the friction coefficient approaches a constant value of approx. 0.25. On the other hand, for braking method B, the situation is almost mirrored. The coefficient of friction is initially slightly below 0.2 and over time approaches an almost constant value of around 0.225. This suggests that higher and more variable particle concentrations could be emitted in the first half of the southbound trip, particularly for braking method A, whereas the emissions get more constant from this point onwards.

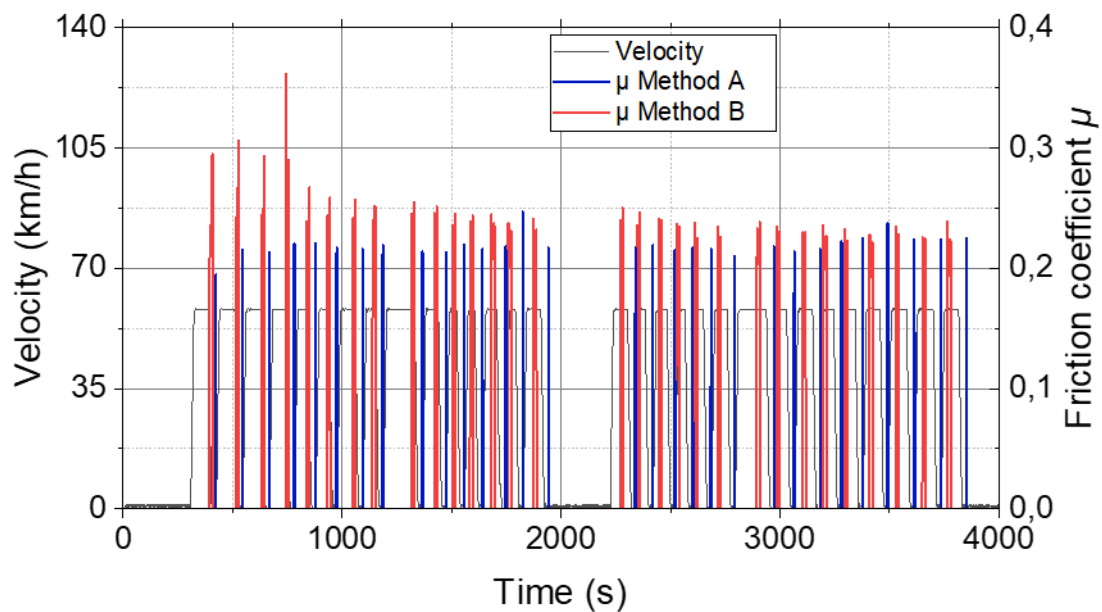


Figure 15: Friction coefficients of the block brake from Sofia for braking method A and B at maximum load

3.4.2.2. RESULTS FROM PHYSICAL AEROSOL CHARACTERISATION

Analysing the brake dust with regard to its particle size distribution is essential also for the brake from Sofia in order to be able to identify a physical tracer. The analysis results for both braking methods and two load cases are therefore presented and discussed in the following chapter. The lengthy running-in of the brake in order to develop a uniform friction surface limited the available measurement time, which is why only size distributions for the minimum and maximum load are available. In order to obtain a first impression of the brake dust emitted by the brake from Sofia compared to the brake system from Lisbon, Figure 16 shows the time series of the particle number concentration obtained from both brakes. They were measured with a condensation particle counter, each during an exemplary test cycle in full load operation and with braking method A. The duration of the entire test cycle, the lengths of the individual sections and the driving speed are different and mimic the local settings in Lisbon and Sofia, respectively. Consequently, the concentration spikes occur at different times.

Nonetheless, from the number concentrations plotted in Figure 16, it is apparent that the type of brake from Sofia emits far fewer particles per braking event in the submicron range ($d_p < 1 \mu\text{m}$). It is also noticeable that the absolute concentration varies less during the braking events. This result could be because the substances contained in the brake pad tend to evaporate less, which means that less ultrafine particles are formed by nucleation. For the brake from Sofia, rather high concentrations peaks are observed during braking operations 5 (approx. 550 s) and 6 (approx. 650 s), although these two braking events did not principally differ from the others. These relatively high number concentrations compared to the remaining braking operations were regularly identified for the southbound trip of the test cycle, but not just only for braking events 5 and 6. The reason for this behaviour is not yet understood. In contrast, no atypical number concentrations like this could be

identified for minimum load operation. This could be an indication that locally high temperatures may play a role for this behaviour.

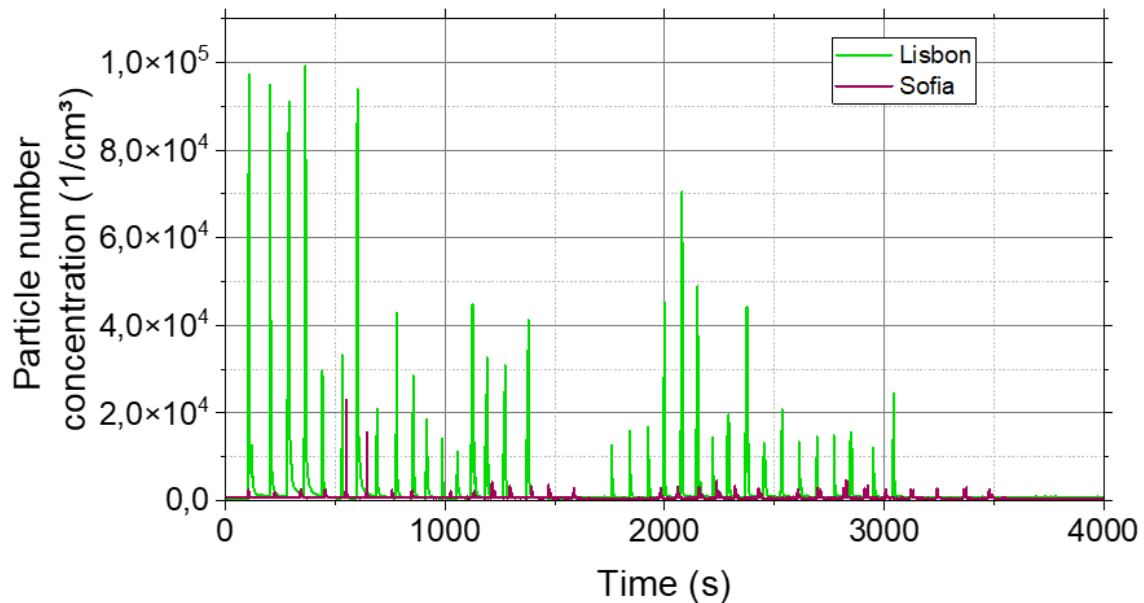


Figure 16: Particle number concentration over the respective test cycle of the brake types used in the metros

In order to be able to investigate this behaviour in more detail, the size distributions at the different operating conditions are shown below. The measurement data were analysed according to the same principle as for the Lisbon brake. Each braking event is initially analysed individually. An average particle size distribution of the brake emissions is calculated over the mechanical braking duration at the individual stations. The background concentration has not been very stable during these experiments. To determine the relevant background contribution, the size distributions, measured during the last 20 seconds before a braking event were averaged and then deducted from the size distributions during the braking events. In this way, the “true” size distribution of the brake dust can be approximated. The average size distributions for braking method A with minimum load and maximum load, respectively, are shown in Figure 17 along with the standard deviations of the concentrations in each size bin.

The graphs show a constant modal diameter at approx. 180 nm, measured with the FMPS. In general, number concentrations were higher, when full load was assumed compared to the minimum load. In contrast, the number size distributions measured with the OPS are almost identical. The constant peak in the narrow size range around 180 nm indicates that particles of this size are released in every metro station of the M1 line with braking method A. The large standard deviations in the range of ultrafine particles clearly reflect the influence of the sometimes much higher number concentrations during the southbound trip in maximum load operation. A potential reason could be very high local temperatures, which do not occur during the test cycle for minimum load.

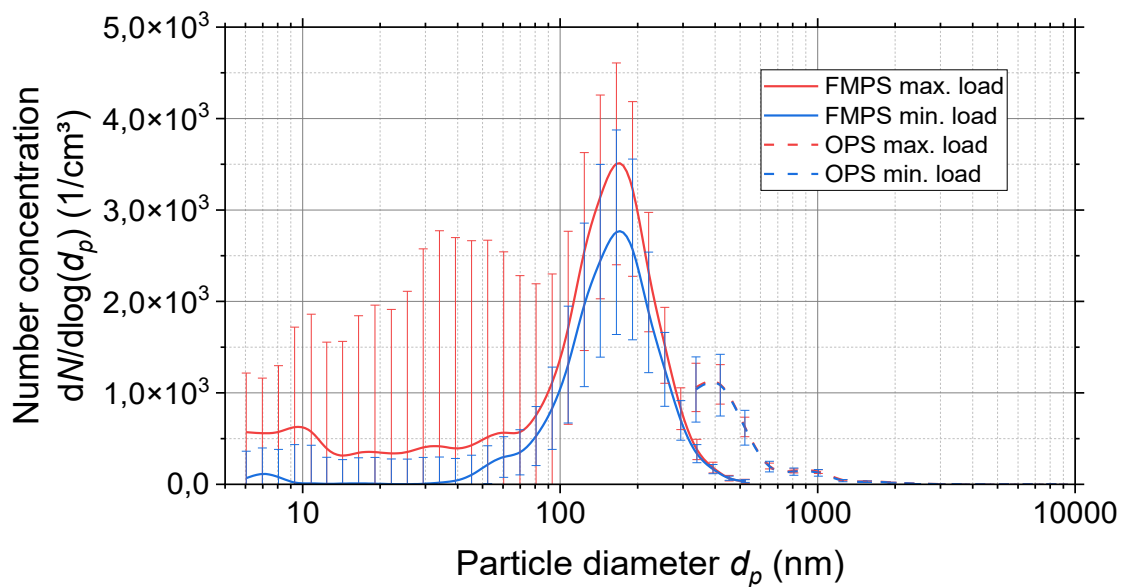


Figure 17: Average brake particle size distribution for braking method A in maximum load operation (red) and minimum load operation (blue)

For the disc brake from Lisbon, it had been observed that the peak concentrations are at approx. 200 nm, emitted with braking method B (approx. 450 1/cm³), were by a factor of around 17 lower than with method A (approx. 7500 1/cm³). The same qualitative trend was observed here for the brake from Sofia. However, due to the generally lower emission from this brake, the concentrations with method B were near or at the noise level and could thus not be quantified. Considering the peak concentration of the brake from Sofia of around 2,500 to 3,500 1/cm³ for the different load cases and assuming a similar ratio between methods A and B, the peak concentrations would be in a range between approximately 150 and 200 1/cm³. Consequently, a coinciding increase of the particle concentration around 180 nm and the brake events could typically not be detected. Accordingly, the size distribution of the brake particles could no longer be distinguished from the size distribution of the background and are therefore not displayed here.

In general, with these low-emissions of the brake, it may be very challenging to identify these particles and measure their concentrations in the station. The rather high operating frequency and the large number of brake units on a train may be beneficial for this purpose, but on the other hand, a large number of trains also increases the emission of particles from other non-brake related sources.

3.4.2.3. RESULTS FROM CHEMICAL AEROSOL CHARACTERISATION

The characterisation of the brake dust has been completed for the metro in Sofia with the goal of determining a chemical tracer element. For this purpose, the quartz fibre filters loaded with brake dust as well as collected abraded material of the brake sole were chemically analysed (ICP-MS and ICP-OES, EC/OC just for filter analysis). The method for determining the mass-related percentages of the elements was carried out as described in chapter 3.3.2.3. Blank filters were also used for the plausibility check. Due to the low emissions, each pair of filters (PM₁₀ & PM_{2.5}) needed to sample the dust during

two entire driving cycles. This allowed a sufficient mass to be collected on the filters in order to exceed the limit of quantification (LOQ) for all relevant chemical elements. However, this was still not sufficient for braking method B, and consequently, the determination of the chemical tracer is only based on the brake dust collected using method A and the brake sole material. It is, however, assumed that the composition does not vary significantly, especially between the two braking methods. The elemental compositions of the brake dust are shown in Figure 18 (PM₁₀) and Figure 19 (PM_{2.5}), each at maximum (left) and minimum (right) load.

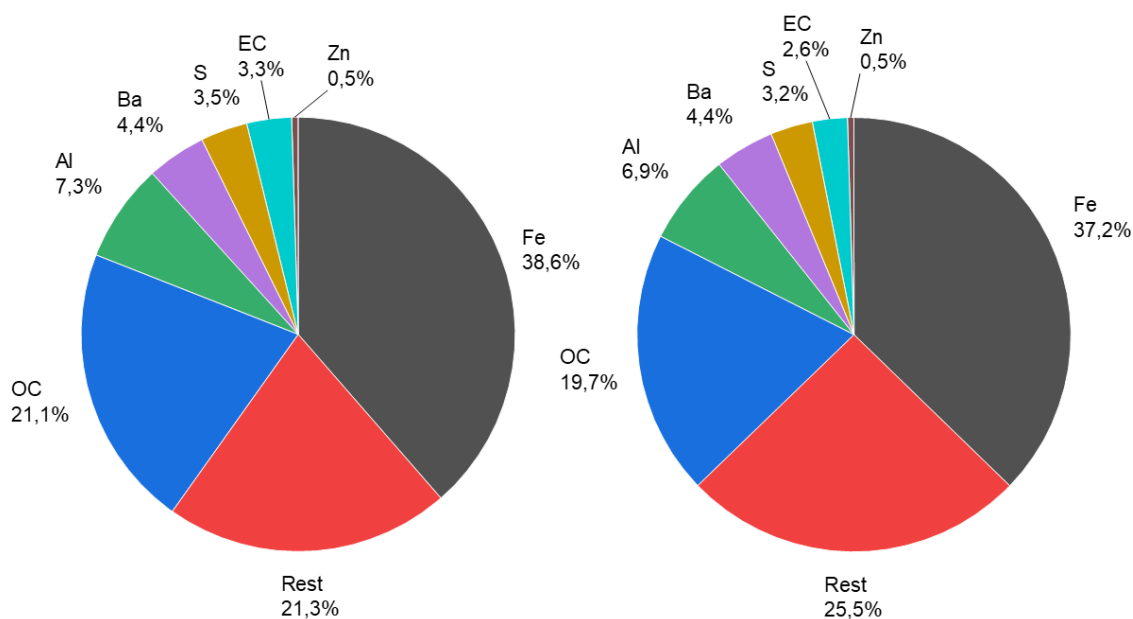


Figure 18: Mass-related composition of PM₁₀ brake dust for braking method A in maximum load operation (left) and minimum load operation (right)

In particular, the elements iron (Fe), aluminium (Al), barium (Ba), sulphur (S) and zinc (Zn) are transferred to the airborne state in descending percentage order. The rest represents all unanalysed elements and elements whose masses on the filters are below the LOQ or elements, whose concentrations were in the range of those in the blank filters. In the previous analyses of the Lisbon brake, it was assumed that the organic carbon (OC) originates from the cooling air. This behaviour can also be confirmed within this measurement campaign, as the collected mass of OC per filter is at a similar level regardless of the operating conditions and the pre-separator. This behaviour naturally manifests itself in an increase in the OC percentage for PM_{2.5} due to the generally lower loading of the filter. The results in Figure 19 for PM_{2.5} brake dust in empty load operation are an exception, as the timer of one of the low volume samplers could only be set by the hour, but the test ran overnight and was therefore approx. 50 minutes longer than the normal duration of the test cycle.

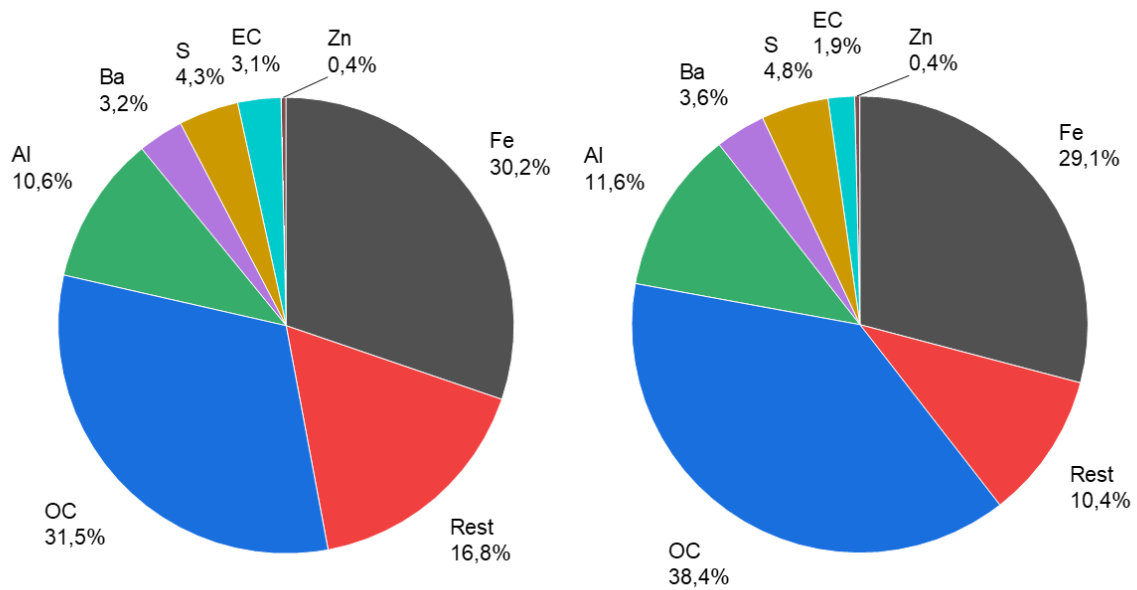


Figure 19: Mass-related composition of PM_{2.5} brake dust for braking method A in maximum load operation (left) and minimum load operation (right)

The elements that are presumably contained in sufficient quantities in the brake dust would therefore be iron, aluminium and barium. It is justified to assume that other particle sources for iron and aluminium can be found in the metro station, e.g. stemming from rail abrasion. For barium, on the other hand, no other sources are known, so that barium is suggested as a suitable chemical tracer for precisely this block brake used in Sofia. Finally, Figure 20 shows the composition of the brake sole material to ensure that barium contained in the analyzed dust really comes from the brake itself.

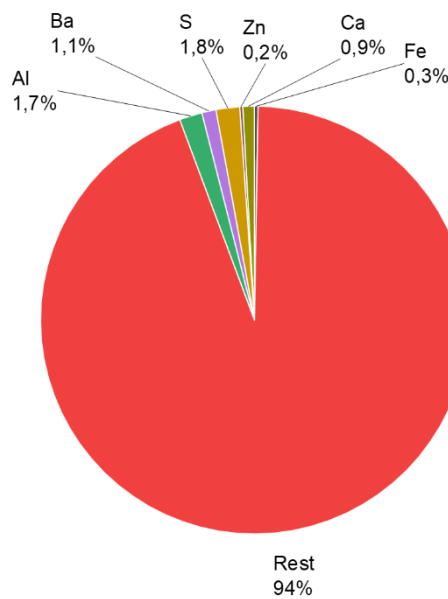


Figure 20: Mass-related composition of the brake sole material

As expected, the metallic content of the pure brake sole material is very low and most elements could not be quantified by the applied analytical methods. Presumably, they are mostly organic. It is all the more surprising that the brake dust itself contains a high percentage of iron. Block brakes with composite brake soles are known to be very maintenance-intensive. The brake soles contain iron fibres, which lead to high abrasion of the running surface. The wheels are usually made of ferrous materials. This behavior could therefore explain the high iron content in the brake dust. Any elements contained in the brake dust can also be detected in the brake pad material. In particular, the analysis result of barium with a percentage of 1.1 % in the material confirms the selection as a chemical tracer for this brake from Sofia. For higher certainty, also the Ba/Fe ratios may be determined as an even clearer source indicator, as suggested in the literature [24, 25].

3.4.3. CONCLUSIONS FROM MEASUREMENTS ON BRAKE FROM METRO SOFIA

The measurements with the block brakes, used by the Metro Sofia revealed that these emit much lower particle concentrations than the disc brakes used by Metro Lisbon. The size distributions were, however, rather similar with a primary modal electrical mobility diameter at around 180 nm (compared with 200 nm for the brake from Lisbon). This particle size is not very abundant in the atmosphere and can therefore be considered as a physical tracer for the measurements at the Opalchenska station. It should, however, be noted that due to the low concentrations emitted during the most realistic braking method B, which in the experiments were mostly at noise level, the detection of these particles at the station may be very challenging, if not impossible. A more promising procedure for an unambiguous distinction between brake dust and background particles is by using a chemical tracer. Unlike the brakes from Lisbon, the dust analysed here did not show any antimony content. Barium can be used instead as a chemical tracer, which is not widely used in other applications, from where barium-containing particles they may become airborne.

3.5. POSSIBLE CONTRIBUTION OF BRAKE EMISSIONS TO WATER QUALITY AND DAMAGE TO HISTORIC BUILDINGS

To this day, the predominant focus of numerous research investigations has been the analysis of the adverse health effects resulting from various ambient air pollutants on human populations. Nevertheless, attention should also be shifted towards assessing the influence of these pollutants on water quality or the structural integrity of building materials within archaeological sites and monuments within urban environments. Although several studies exist for the effect of general air pollutants, no study could be identified, explicitly addressing effects of brake dust emissions from metro trains. The following literature review therefore includes data for general air pollutants and tries to read across to obtain information on possible effects of brake dust.

A noteworthy reduction in emissions is reported by the European Environment Agency, from a cumulative 65 million tons in 1990 to approximately 20 million tons in 2021 [26]. However, the concerning issue persists and corrosion to monuments from chemical exposure and soiling induced by suspended particles not only generates economic losses, but more significantly contributes to the deterioration of modern's society cultural heritage [27]. Since it is known that brake dust emissions contain significant amounts of metallic particles, this effect may even be pronounced. However, as long as the emissions occur mainly in the metro tunnel with relatively little air exchange to the outside, this effect is expected to be rather low, unless the metro stations themselves are considered as historic and/or cultural heritage.

Soiling, frequently also referred to as ‘black soiling’, is the darkening visual change of exposed building surfaces, resulting from the accumulation of particulate matter. Particulate elemental carbon (EC), also known as black carbon or graphitic carbon, is reported to be the principal compound responsible for soiling. Primary sources of PEC involve road traffic emissions such as diesel emissions, wood burning and various other forms of incomplete combustions of fossil fuels that lead to the generation of carbonaceous fine particles [28]. This effect is not considered to be applicable to brake dust emissions from metro trains as the measurements shown above do not indicate major emissions of EC.

In addition to soiling, the degradation of surfaces on historical buildings and monuments is greatly influenced by air pollution. The impact of ambient pollutants such as sulphur oxides (SO_x) and sulphates, nitrogen oxides (NO_x) and nitrates, chlorides, carbon dioxide (CO₂), ozone, and particulate matter released into the atmosphere and subsequently, deposited on diverse materials like stones and ferrous metals [29] exhibits both substantial and often irreversible effects. Biological factors also contribute to this phenomenon and water in particular assumes a twofold role. It can function both as a solvent agent with the capability to solubilize components like calcium carbonate or gypsum and as a conduit for transporting salts and/or other pollutants onto the stone surfaces or within its porous structure, which often leads to subsequent deterioration of the architectural material [30]. The aforementioned pollutants react with water in precipitation and for instance SO_x on calcareous stones can lead to the formation of CaSO₄ (gypsum) which in combination with particulate matter is deposited on the exterior of monuments and buildings and results to the formation of black crusts. Upon the oxidation of nitrogen dioxide (NO₂) to generate dinitrogen pentoxide (N₂O₅), the latter reacts with water producing nitric acid (2HNO₃). This substance, in turn, further contributes to the corrosion of stone substrates. Since brakes do not emit significant amounts of gases, this process appears negligible.

The mechanisms of decay are primarily investigated in two distinct ways: 1) the study of material damage resulting from dry deposition of pollutants, and 2) the examination of damage through wet deposition. Dry deposition is the direct transfer of gases and particulates onto various surfaces, whereas wet deposition involves the transportation of airborne pollutants in an aqueous form such as through precipitation like rain, snow, or fog [31]. As already mentioned, given that water acts as a reactant and a solvent, wet deposition is considered as a swifter and more efficacious process in regards of the damage induced. Increased levels of SO₂ and NO_x emissions from vehicles with internal combustion engines, agriculture, industry, coal consumption and other anthropogenic sources have resulted in frequent acidic precipitations especially in highly dense urban areas and countries [32]. Despite the reported buffering and, in certain cases, neutralizing properties of particulate matter against acidic precipitation [33], multiple studies have consistently demonstrated that PM_{2.5} particles can effectively transport acidic aerosols. Through wet deposition, these particles accumulate on structures or aquatic ecosystems causing severe deterioration and a decline in environmental quality [34, 35]. Wet deposition of brake dust may, however, only occur if the train is operated outside the tunnel, which is hence outside of the scope of this task, which focusses on emissions in the (semi-) closed environment of a metro tunnel or station.

Bioindicators, such as different genotypes of fish, always served as model species in various investigations aiming at examining the potential harmful effects of pollutants, which aside from their negative impact on animal life, may also pose a risk to human health [36, 37]. In their research, Gokul et al. [38] examined the effects of PM₁₀ to zebrafish embryos and zebrafish larvae. They reported reduced vascular and neurovascular development, delay of embryonic development, alteration of gene expression, decreased rate of heartbeat, obstruction of blood flow, and increased mortality rate.

In regards of PM_{2.5} effects on zebrafish, they continued by reporting a significant zebrafish mortality, morphological alterations of the organs such as eyes, gills, livers, brains and hearts, intestine necrosis, and cardiac abnormalities and DNA damage to zebrafish embryos. In addition to fish, other aquatic species such as water snails have also been reported to exhibit adverse effects under exposure to pollutants and particulate matter. In an attempt to assess the movement and kinetic behaviour, Hartono et al. [39] conducted experiments on the freshwater snail *Parafossarulus striatulus* subjecting it to high (7.75 mg/L) and low (3.88 mg/L) concentrations of PM_{2.5} in parallel with high acidity (pH 5.0) and metal components such as aluminium (Al), lead (Pb) and zinc (Zn)-compounds commonly present in PM_{2.5}. High concentrations of PM_{2.5} negatively impacted the movement and overall behaviour of *Parafossarulus striatulus*. In addition, sulphuric acid aerosols and aluminium were found to exhibit the most negative effects. Out of these relevant elements, only zinc was found in the emitted dust (see Figure 9). Whereas no aluminium was found in the investigated brakes, this may change in the future, because the use of aluminium instead of cast iron brake discs is a very promising ongoing development for passenger cars that shall reduce PM emissions while offering superior performance and durability [40, 41].

In recent studies [42, 43], the investigation of settleable particulate matter (SePM) has emerged as a subject of great interest, given its complex composition involving particles of diverse sizes and constituents like metals, nanoparticles, and organic and inorganic compounds [38]. These studies raise questions regarding the dissociation and fragmentation of these agglomerates within aqueous media. SePM is able to contribute to water contamination through two primary pathways: firstly, by settling on water surface, undergoing dispersion, and converting into nanoparticles smaller than 200 nm, thereby serving as a direct source of metal nanoparticles contamination; and secondly, by gradually assimilating in cells, tissue and bloodstream of aquatic species [42, 44]. In the research conducted by Da Souza et al. [42], samples were collected within the vicinity of steel and iron industry. The obtained samples were subsequently categorized into eight fractions spanning from 425 to ≤ 10 μm and their characterization was undertaken based on their physical and chemical properties. The findings of the study unveiled that metallic nanoparticles combined with salt, silica and other heavy metals formed agglomerates, characterized as SePM on a macroscopic scale. Further analyses indicated that SePM was able to dissociate in water, thereby generating nanoparticles. This phenomenon can contribute to water pollution, with ramifications extending to significant ecological instability and genetic alterations among fish and other aquatic species. Whether this finding is relevant for particles emitted from metro brakes cannot be answered here, because the particle size range covered in our measurements only extends up to 10 μm . Nonetheless, since such large particles have a rather short lifetime in the atmosphere due to their high settling velocities, the described may only be relevant at all, if a metro train brakes close to a body of water. This, in turn, may only occur outdoors and is thus beyond the scope of this task.

In summary, as of now a comprehensive study on the effect of brake dust from metro trains on historic buildings or aquatic systems does not seem to exist. Cross-reading from other studies showed that especially wet deposition of airborne particles is a major source of concern for damage to buildings and transfer of PM to surface and ground water. In order for particles emitted from metro brakes in the (semi-) closed environment of a metro tunnel or station to be wet deposited, they would first need to escape from the semi-closed environment. Although little is known about the air exchange between the tunnel and the environment, it can be speculated that the total amount of brake dust particles emitted from a tunnel into the atmosphere is rather low. The effect is likely much larger when the



trains are operated in the open environment, i.e. outside of the metro tunnel, but these scenarios are out of scope of this task.

4. DEVIATIONS FROM THE PLAN

In terms of content, the measurements were carried out as planned, however, the measurements on the brakes from Sofia were severely delayed, due to the late delivery of the original brake components. The delay was caused by the shortage of spare and wear parts, like the wheel and brake pad for these trains, so that Metro Sofia initially did not want to hand over the parts as a precautionary measure. It should be noted that the trains run on this particular line (M1) are Russian made and that the required parts are still only produced in Russia. The current sanctions and trade restrictions against led to this situation. Eventually the measurements were carried out in spring 2024.

During the entire process there were frequent discussions between IUTA and CSIC to assure a smooth flow of all information necessary for carrying out the measurements at the station, e.g. concerning the physical and chemical tracers for the two different brakes. All relevant results for the brake from Lisbon were shared before the measurements at the *Alto dos Moinhos* station commenced. Similarly, the results for the brake from Sofia have also been shared early on and before the submission of this deliverable report, even though the measurements in the *Opalchenska* station are still pending at the time of writing of this deliverable report. This ensured that all necessary data are available, when the measurements in Sofia will commence. Consequently, the delay in the measurement of the brake dust emissions and writing of the deliverable report did not affect the work in any other (sub-) work package.

5. LINKS WITH OTHER WPS

The main users of the results from this work are within WP3, in particular in task 3.3 in which the efficacy of the air cleaners in semi-closed environments, shall be determined in metro stations like *Opalchenska* and *Alto dos Moinhos*.

Further users of the results are in work package 4, particularly for the life cycle analysis and the assessment of worker exposure.

Additional links exist to WP2, in which the emissions from bus brakes are measured on a different dynamometer test rig, but using a very similar set up. IUTA is a partner in both work packages and assures a smooth knowledge transfer between the work packages.

6. CONCLUSIONS AND RECOMMENDATIONS

The emissions from two different metro brakes, a disc brake as used by Metro Lisbon and a block brake as used by Metro Sofia, have been characterised and suitable physical and chemical tracers identified. These tracers are a particle size of around 200 nm (electrical mobility equivalent diameter) and antimony as a non-abundant chemical compound for the brakes from Lisbon, and a size of approximately 180 nm and barium as a chemical tracer for the brake from Sofia. It is thus recommended that these concentrations of these tracers are measured in the stations in Lisbon and Sofia, respectively, with the air cleaners on and off. The specific air cleaner efficacy for brake dust can be determined by means of the ratio of the concentrations with the air cleaner switched off and on, respectively.

It should, however, be noted that modern metro trains use a braking method, in which solely the electrical brake is used at higher velocities and the friction brake is only applied below 10 or less km/h for the train to come to a full stop. The emissions measured with this braking method were rather low, which on the one hand means that human exposure to brake dust at metro stations is in general rather low. On the other hand, it makes it challenging to detect the tracer concentrations in the metro stations. This is particularly true for the time-resolving measurements of the number size distributions. For the determination of the concentrations of the chemical tracer, it is recommended to use a filter sampler with a high flow rate and to sample over a sufficient period of time in order to collect sufficient material for analysis. However, assuming that the chosen air cleaners employ filters with a high and nearly constant efficiency over all particle sizes, it may also be a reasonable guess to assume that brake dust concentrations at the respective station are reduced with the same efficiency as total dust concentration (e.g. in terms of PM_{2.5})

The literature review on the effect of brake dust emitted by metro trains on air and water quality and on damages to historic buildings revealed that this is still an under-researched topic. Cross reading from other papers revealed that the effect on ambient air and water quality can be expected to be rather low, due to the low air exchange rates of metro tunnels. The same applies to the effect on historic buildings, unless the metro station itself is considered to be one. These judgements are certainly very different for the brake dust emissions that occur over ground, when the dust is emitted directly into the atmospheric and/or aqueous environment. The entire scenario would change when the air ventilation rate is technically increased. This would certainly improve the air quality inside the tunnel but transport the dust to the outdoors, where it may impart the air and water quality or deposit on historic buildings. It is therefore recommended to equip technical ventilation systems of metro tunnels with exhaust filtration systems.

7. BIBLIOGRAPHY

- [1] D. Dockery, "Health Effects of Particulate Matter," *Annals of Epidemiology*, vol. 19, pp. 257-263, <https://doi.org/10.1016/j.annepidem.2009.01.018>, 2009.
- [2] C. Pope III and D. Dockery, "Health effects of fine particulate air pollution: Lines that connect," *Journal of the Air & Waste Association Management Association*, no. 56, pp. 709-742; <https://doi.org/10.1080/10473289.2006.10464485>, 2006.
- [3] D. Dockery, A. Pope, X. Xu, J. Spengler, J. Ware, M. Fay, B. Ferris and F. Speizer, "An association between air pollution and mortality in six U.S. cities," *The New England Journal of Medicine*, no. 329, pp. 1753-1759, DOI: 10.1056/NEJM199312093292401, 1993.
- [4] F. Karagulian, B. C.A., C. Dora, A. Prüss-Ustün, S. Bonjour, H. Adair-Rohani and M. Amann, "Contributions to cities' ambient particulate matter (PM): A systematic review of local source contributions at global level," *Atmospheric Environment*, vol. 120, pp. 475-483, 2015.
- [5] H. van der Goon, J. Hulskotte, M. Joczwicka, R. Kranenburg, J. Kuenen and A. Visschedijk, "European emission inventories and projections for road transport non-exhaust emissions," in *Non-Exhaust Emissions (Ed. F. Amato)*, Elsevier, London, 2018, pp. 101-121.
- [6] R. Harrison, A. Jones, J. Gietl, J. Yin and D. Green, "Estimation of the contributions of brake dust, tire wear and resuspension to nonexhaust traffic particles derived from atmospheric measurements," *Environmental Science & Technology*, vol. 46, pp. 6523-6529, 2012.
- [7] P. Aarnio, T. Tuomi, A. Kousa, T. Mäkelä, A. Hirsikko, K. Hämeri, M. Räisänen, R. Hillamo, T. Koskentalo and M. Jantunen, "The concentrations and composition of and exposure to fine particles PM_{2.5}) in the Helsinki subway system," *Atmospheric Environment*, vol. 39, pp. 5059-5066, 2005.
- [8] M. Cusack, N. Talbot, J. Ondráček, M. Minguillón, V. Martins, K. Klouda, J. Schwarz and V. Zdímal, "Variability of aerosols and chemical composition of PM₁₀, PM_{2.5} and PM₁ on a platform of the Prague underground station," *Atmospheric Environment*, vol. 118, pp. 176-183, 2015.
- [9] T. Moreno, X. Querol, V. Martins, M. Minguillón, C. Reche, L. Ku, H. Eun, K. Ahn, M. Capdevila and E. de Miguel, "Formation and alteration of airborne particles in the subway environment," *Environmental Science - Processes & Impacts*, vol. 19, p. 59, 2017.
- [10] T. Moreno, V. Martins, X. Querol, T. Jones, K. BéruBe, M. Cruz Minguillón, F. Amato, M. Capdevila, A. de Miguel, S. Centelles and W. Gibbons, "A new look at inhalable metalliferous airborne particles on railway subway platforms," *Science of the Total Environment*, vol. 505, pp. 367-375, 2015.
- [11] T. Grigoratos and G. Martini, "Brake wear particle emissions - A review," *Environmental Science and Pollution Research*, vol. 22, pp. 2491-2504, 2015.

- [12] A. Thorpe and R. Harrison, "Sources and properties of non-exhaust particulate matter from road traffic: A review," *Science of the Total Environment*, vol. 400, pp. 270-282, 2008.
- [13] C. Asbach, A. Todea, M. Zessinger and H. Kaminski, "Entstehung und Möglichkeiten zur Messung von Fein- und Ultrafeinstaub beim Bremsen," in *XXXVII. Internationales μ -Symposium 2018 - Bremsen-Fachtagung (Hrsg. Ralph Mayer)*, Berlin, Springer Vieweg, 2018, pp. 45-67.
- [14] H. Niemann, H. Winner, C. Asbach, H. Kaminski, G. Frenz and R. Milczarek, "Influence of disc temperature on ultrafine, fine and coarse particle emissions of passenger car disc brakes with organic and inorganic pad binder materials," *Atmosphere*, vol. 11, p. 1060, 2020.
- [15] O. Nosko, J. Vanhanen and U. Olofsson, "Emission of 1.3-10 nm airborne particles from brake materials," *Aerosol Science and Technology*, vol. 51, pp. 91-96, 2017.
- [16] T. Grigoratos, M. Mathissen, R. Vedula, A. Mamakos, C. Agudelo, S. Gramstat and B. Giechaskiel, "Interlaboratory study on brake particle emissions - Part I: Particulate matter mass emissions," *Atmosphere*, vol. 14, p. 498, 2023.
- [17] M. Mathissen, T. Grigoratos, S. Gramstat, A. Mamakos, R. Vedula, C. Agudelo, J. Grochowicz and B. Giechaskiel, "Interlaboratory study on brake particle emissions Part II: Particle number emissions," *Atmosphere*, vol. 14, p. 424, 2023.
- [18] M. Mathissen, J. Grochowicz, C. Schmidt, R. Vogt, F. Farwick zum Hagen, T. Grabiec, H. Steven and T. Grigoratos, "A novel real-world braking cycle for studying brake wear particle emissions," *Wear*, Vols. 414-415, pp. 219-226, 2018.
- [19] F. Keller, L. Krupa, A. Beck, T. Wörz, B. Weller, K. Kohn, S. Pfannkuch, T. Jessberger, M. Lehmann and S. Ashish, "Development of a Modeling Approach to Numerically Predict Filtration Efficiencies of Brake Dust Particle Filters," *SAE Technical Paper*, pp. 2021-01-1285, 2021.
- [20] M. Hascoet and L. Adamczak, "At source brake dust collection system," *Results in Engineering*, vol. 5, p. 100083, 2020.
- [21] EN, *DIN EN 12341:2023-10: Außenluft - Gravimetrisches Standardmessverfahren für die Bestimmung der PM₁₀- oder PM_{2,5}-Massenkonzentration des Schwebstaubes*, Berlin: Beuth Verlag, 2023.
- [22] N. Buckowiecki, P. Lienermann, M. Hill, R. Figi, A. Richard, M. Furger, K. Rickers, G. Falkenberg, Y. Zhao, S. Cliff, A. Prevot, U. Baltensperger, B. Buchmann and R. Gehrig, "Real-world emission factors for antimony and other brake wear related trace elements: Size segregated values for light and heavy duty vehicles," *Environmental Science and Technology*, vol. 43, pp. 8072-8078, 2009.
- [23] O. von Üexküll, S. Skerfvong, R. Doyle and M. Braungart, "Antimony in brake pads - a carcinogenic component?," *Journal of Cleaner Production*, vol. 13, pp. 19-31, 2005.
- [24] K. Van Ryswyk, A. T. Anastasopoulos, G. Evans, L. S. K. Sun, R. Kulka, L. Wallace and S. Weichenthal, "Metro commuter Exposures to particulate air pollution and PM_{2.5} - Associated elements in

- three Canadian cities: The urban transportation exposure study,” *Environmental Science & Technology*, no. 51, pp. 5713-5720, 2017.
- [25] K. Van Ryswyk, R. Kulka, C.-H. Jeong, A. T. Anastasopoulos, T. Shin, P. Blanchard, D. Veikle and G. J. Evans, “Sources of subway PM_{2.5}: Investigation of a system with limited mechanical ventilation,” *Transportation Research D*, vol. 133, p. 104164, 2024.
- [26] EEA - European Environmental Agency, “Air pollution in the EU,” 17 11 2023. [Online]. Available: <https://www.consilium.europa.eu/de/infographics/air-pollution-in-the-eu/>. [Accessed 18 12 2023].
- [27] T. Grøntoft, “Estimation of Damage Cost to Building Façades per kilo Emission of Air Pollution in Norway,” *Atmosphere*, vol. 11, p. 686, 2020.
- [28] C. Grossi, R. Esbert, F. Díaz-Pache and F. Alonso, “Soiling of building stones in urban environments,” *Building and Environment*, vol. 38, pp. 147-159, 2003.
- [29] R. Butlin, “Effects of air pollutants on buildings and materials,” *Proceedings of the Royal Society of Edinburgh, Section B: Biological Sciences*, vol. 97, pp. 255-272, 1990.
- [30] S. A. Ruffolo, M. F. La Russa, N. Rovella and M. Ricca, “The Impact of Air Pollution on Stone Materials,” *Environments*, vol. 10, p. 119, 2023.
- [31] C. Saiz-Jimenez, “Deposition of airborne organic pollutants on historic buildings,” *Atmospheric Environment. Part B. Urban Atmosphere*, vol. 27, pp. 77-85, 1993.
- [32] W. Wu and Y. Zhang, “Effects of particulate matter (PM_{2.5}) and associated acidity on ecosystem functioning: response of leaf litter breakdown,” *Environmental Science and Pollution Research International*, vol. 25, p. 30720–30727, 2018.
- [33] W. Wang, H. Liu, X. Yue, H. Li, J. Chen, L. Ren, D. Tang, S. Hatakeyama and A. Takami, “Study on acidity and acidic buffering capacity of particulate matter over Chinese eastern coastal areas in spring,” *Journal of Geophysical Research: Atmospheres*, vol. 111, p. D18207, 2006.
- [34] K. He, Q. Zhao, Y. Ma, F. Duan, F. Yang, Z. Shi and G. Chen, “Spatial and seasonal variability of PM_{2.5} acidity at two Chinese megacities: insights into the formation of secondary inorganic aerosols,” *Atmospheric Chemistry and Physics*, vol. 12, pp. 1377-1395, 2012.
- [35] J. Xue, A. K. Lau and J. Z. Yu, “A study of acidity on PM_{2.5} in Hong Kong using online ionic chemical composition measurements,” *Atmospheric Environment*, vol. 45, pp. 7081-7088.
- [36] C. Faggio, P. G., S. Marafioti, F. Arfuso, G. Fortino and F. Fazio, “Metabolic response to monthly variations of *Sparus aurata* reared in mediterranean off-shore tanks,” *Turkish Journal of Fisheries and Aquatic Sciences*, pp. 567-574, 2014.
- [37] F. Hashempour-Baltork, B. Jannat, B. Tajdar-Oranj, M. Aminzare, H. Sahebi, A. Mirza Alizadeh and H. Hosseini, “A comprehensive systematic review and health risk assessment of potentially toxic

- element intakes via fish consumption in Iran,” *Ecotoxicology and Environmental Safety*, vol. 249, p. 114349, 2023.
- [38] T. Gokul, K. Kumatr, P. Prema, A. Arun, P. Balaji and C. Faggio, “Particulate pollution and its toxicity to fish: An overview,” *Comparative Biochemistry and Physiology. Toxicology & Pharmacology*, vol. 270, p. 109646, 2023.
- [39] D. Hartono, B. Lioe, Y. Zhang, B. Li and J. Yu, “Impacts of particulate matter (PM2.5) on the behavior of freshwater snail *Parafossarulus striatulus*,” *Scientific Reports*, vol. 7, p. 644, 2017.
- [40] N. Kumar, A. Bharti, H. Goyal and K. Patel, “The evolution of brake friction materials: A review,” *Materials Physics and Mechanics*, vol. 47, pp. 796-815, 2021.
- [41] P. Kumar and S. Gnanaraj, “Aluminium-Silicon based metal matrix composites for brake rotor applications: a review,” *Engineering Research Express*, vol. 5, p. 022002, 2023.
- [42] I. De Souza, M. Morozesk, M. Bonomo, V. Azevedo, M. Sakuragui and M. e. a. Elliot, “Differential biochemical responses to metal/metalloid accumulation in organs of an edible fish (*Centropomus parallelus*) from neotropicaestuaries,” *Ecotoxicology and Environmental Safety*, vol. 161, pp. 260-269, 2018.
- [43] L. Goswami, K.-H. Kim, A. Deep, P. Das, S. Bhattacharya, S. Kumar and A. Adelodun, “Engineered nano particles: Nature, behavior, and effect on the environment,” *Journal of Environmental Management*, vol. 196, pp. 297-315, 2017.
- [44] E. Panzarini, S. Mariano, E. Carata, F. Mura, M. Rossi and L. Dini, “Intracellular Transport of Silver and Gold Nanoparticles and Biological Responses: An Update,” *International Journal of Molecular Sciences*, vol. 19, p. 1305, 2018.